Journal of Scientific Computing manuscript No.
(will be inserted by the editor)

A High–Order Perturbation of Envelopes (HOPE) Method for Electromagnetic Scattering by Periodic Inhomogeneous Chiral Media

David P. Nicholls · Liet Vo

Received: date / Accepted: date

Abstract Chirality plays an important role in many optical phenomena and it is crucial to have efficient and accurate numerical algorithms to simulate solutions in this setting. In this paper we discuss a High–Order Spectral algorithm, coupled to geometric regular perturbation theory, which results in just such a method. We view the chirality of the laterally periodic, constant permittivity/permeability structure as deviating from a background value, and demonstrate analyticity of the field scattered by a plane electromagnetic wave with respect to this deformation. This analyticity is not only with respect to chirality perturbations of arbitrarily large real size, but also joint in the spatial variables. We also show how the High–Order Perturbation of Envelopes (HOPE) recursions which we used to establish these results can be implemented as a rapid, robust, and reliable numerical algorithm.

Keywords Linear wave scattering, Helmholtz equations, inhomogeneous media, layered media, high–order spectral methods, high–order perturbation of envelope methods.

Mathematics Subject Classification (2020) 65N35, 78M22, 78A45, 35J25, 35Q60, 35Q86

David P. Nicholls
Department of Mathematics, Statistics, and Computer Science,
University of Illinois at Chicago,
Chicago, IL 60607, U.S.A.
E-mail: davidn@uic.edu

Liet Vo
School of Mathematical and Statistical Sciences,
The University of Texas Rio Grande Valley,
Edinburg, TX 78539, U.S.A.
E-mail: liet.vo@utrgv.edu

1 Introduction

Chirality is a crucial property in chemistry [14], biology [53], and physics [7] which occurs in nature (e.g., hands, shells, amino acids, DNA/RNA) and has been exploited by humans to great advantage (e.g., gloves, spiral staircases, screws). A chiral object is one that cannot be superposed onto its reflection (enantiomer), with the classic example being a hand (whose Greek name gives us the term "chiral") leading to the natural classification of such an object by its "handedness." Sometimes, enantiomers (an object and its reflection) exhibit quite different behaviors, with a most tragic example giving rise to the thalidomide disaster of the late 1950s and early 1960s [64]. Thalidomide has two non-superposable enantiomers: (S) which is teratogenic and (R) which is therapeutic [11]. In the 1950s, the latter was administered to animals and the successful experiments led to its rapid prescription in humans, notably pregnant women for treatment of morning sickness. However, in humans this enantiomer rapidly interconverts *in vivo* leading to disastrous consequences. The long–standing "thalidomide paradox" is why this racemization of thalidomide in humans but not the experimental trial animals? Tokunaga *et al* [64] put forward a hypothesis, but, regardless of the resolution, it is clearly of the highest importance to be able to discriminate amongst enantiomers of chemical species. (Notably, the reputation of thalidomide has been rehabilitated in recent years with the discovery of its beneficial effects in treating leprosy and certain types of cancers [22].)

For this reason we take up the crucially important question of the sensitive and robust detection of chiral molecules [66], though our developments can be applied to more general scenarios involving the optical response of chiral materials; see Mun *et al* [45] and Khaliq *et al* [29] for instance. Regarding chiral sensors, Wang *et al* [66] provide an exhaustive overview of a number of different strategies with the common theme being that great advantage can be gained by incorporating chirality into the sensor itself. Amongst the many schemes outlined, and of particular interest to us, are the ones utilizing (surface) plasmonic responses. For instance, those based upon chiral metasurfaces formed from chiral gold nanorods [37], chiral gold nanorods in a palladium nanostructure [38], arrays of chiral gold helicoid crystals [31], and chiral nanoparticles exhibiting localized surface plasmon resonances (LSPRs) [26]. A particularly compelling application of a Surface Plasmon Resonance (SPR) sensor based upon chiral gold nanorods is given in Kumar *et al* [33] who use it to detect Parkinson's disease.

While there are several approaches to building an SPR sensor [24], a convenient and widely used method is to periodically pattern a structure at the nanoscale. This precise patterning gives one path to overcoming the momentum mismatch required to excite a surface plasmon [56,39,16]. For this reason we focus our attention upon the interaction of linear electromagnetic waves with laterally periodic structures which, of course, arise in many other areas in science and engineering (e.g., underwater acoustics [63], remote sensing [65], and nondestructive testing [60]).

With the overwhelming technological importance of these periodically patterned devices, it is not surprising to learn that the entire host of classical numerical schemes has been brought to the task of their simulation [19]. More specifically, in the context of electromagnetic scattering, one can consider the Finite Difference Time Domain (FDTD) [62] and Finite Difference Frequency Domain (FDFD) methods [58], the Discontinuous Galerkin (DG) [13] and Finite Element Methods (FEM) [27], the Volume Integral Equation (VIE) algorithm [40], and the Discrete Dipole Approximation [15]. More specifically for electromagnetics applications are the Rigorous Coupled–Wave Analysis (RCWA) method [42,43,36], the Fourier Modal Method (FMM) [30], and Planewave Eigensolvers [41,28].

As we shall see, the response of a chiral medium to illumination by linear electromagnetic waves is not well–modeled by the classical constitutive relations. Several alternative models have been put forth and the Drude–Born–Federov (DBF) relations (1) are a popular choice [35,34] that we pursue. The resulting PDEs require specialized treatment and a number of authors have made significant contributions to a rigorous weak formulation of the problem and its subsequent FEM/BEM simulation [61]. We point out early papers on bounded chiral obstacles in two and three dimensions [57,6,5], but the careful rigorous analysis for the periodic gratings we consider began with the pioneering work of Ammari & Bao [1–3]. This was later pursued by Zhang and collaborators for bounded obstacles and periodic gratings [69,70,68]. While not the topic of our current investigations, there have been additional developments on the inverse problem of detecting a chiral obstacle given far field measurements (see [44,20,55] and [46,18,23]).

In this paper we take a slightly different approach to the numerical simulation of periodic chiral structures, which follows the High–Order Perturbation of Envelopes (HOPE) methodology we developed for solving the Helmholtz equation [47] and Maxwell equations [52,51] which arise in scattering from achiral media. As in [47], we focus on y–invariant structures illuminated transversely so that the solution of a scalar Helmholtz equation delivers the vectorial scattered field; see § 4.3. (We will return to the more general three–dimensional case in future work.) This algorithm takes a perturbative point of view by considering chirality functions, $\chi(x, z)$ (see § 2), which are laterally periodic deviations from a trivial one, e.g.,

$$\chi(x, z) = \bar{\chi} - \delta X(x, z), \quad X(x + d, z) = X(x, z),$$

where X is the chirality "envelope," and then conducts regular perturbation theory. As in our previous work [47,52,51] we will show that the scattered field depends *analytically* upon the parameter δ by directly estimating its m–th Taylor correction in appropriate Sobolev spaces. By modifying the nature of our deformation slightly we will rigorously demonstrate that this region of analyticity contains a neighborhood of the *entire* real axis (giving an analytic continuation of our results), and that the field depends *jointly* analytically in both perturbation and spatial variables. Finally, we will show how the resulting recursions can be numerically approximated to deliver a numerical algorithm of impressive accuracy and reliability.

The paper is organized as follows: In § 2 we present the governing equations with a discussion of the DBF constitutive relations that model the chiral effects. In § 3 we describe the transparent boundary conditions we utilize to not only enforce the outgoing nature of the scattered waves, but also truncate the problem to one of finite extent. In § 4 we outline considerations special to chiral layers including a discussion of decoupling the governing equations by polarization in § 4.1, the Beltrami equations which govern these polarizations in § 4.2, and the scalar Helmholtz equations which the transverse components satisfy in § 4.3. In § 5 we derive our HOPE recursions in this context, while, in preparation for our theoretical developments, we define our function spaces in § 6. We rigorously establish analyticity and analytic continuation in § 7, while we prove joint analyticity in § 8. We close with our numerical results in § 9 with discussion of our implementation in § 9.1 and the triply layered medium problem we consider in § 9.2. In § 9.3 we present results of the approximations produced by our implementation as compared to the exact solution of the triply layered model. While this shows convergence, we revisited these in § 9.4 in the context of smoothed solutions to display the aspirational exponential rate of convergence of our algorithm. In § 10 we give concluding remarks and future directions.

2 Governing Equations

We consider structures whose response to illumination by electromagnetic radiation is modeled by the the time–harmonic Maxwell equations (time dependence $\exp(-i\omega t)$ factored out), in the absence of currents and sources,

$$\begin{aligned} \nabla \times E - i\omega B = 0, &\quad \operatorname{div}[B] = 0, \\ \nabla \times H + i\omega D = 0, &\quad \operatorname{div}[D] = 0, \end{aligned}$$

among the electric displacement, D, the magnetic induction, B, the electric field, E, and the magnetic field, H, [25]. To both model the effects of chirality and close the Maxwell equations, we specify the Drude–Born–Fedorov (DBF) constitutive relations

$$D = \epsilon(x,y,z)\left\{E + \chi(x,y,z)\nabla \times E\right\}, \tag{1a}$$

$$B = \mu(x,y,z)\left\{H + \chi(x,y,z)\nabla \times H\right\}, \tag{1b}$$

[35,34]. These equations feature parameters which measure the electric, magnetic, and chiral responses, namely the permittivity, $\epsilon(x,y,z)$, the permeability, $\mu(x,y,z)$, and the chirality, $\chi(x,y,z)$. With these the Maxwell equations now read (with the (x,y,z) dependence suppressed)

$$\begin{aligned} \nabla \times E - i\omega\mu\left\{H + \chi\nabla \times H\right\} = 0, \\ \nabla \times H + i\omega\epsilon\left\{E + \chi\nabla \times E\right\} = 0. \end{aligned}$$

It is very useful to find formulas for the curls of the electric and magnetic fields in terms of these fields themselves. Writing these Maxwell equations as

$$\begin{pmatrix} 1 & -i\omega\mu\chi \\ i\omega\epsilon\chi & 1 \end{pmatrix} \begin{pmatrix} \nabla \times E \\ \nabla \times H \end{pmatrix} = \begin{pmatrix} i\omega\mu H \\ -i\omega\epsilon E \end{pmatrix},$$

we can solve for $\nabla \times E$ and $\nabla \times H$, yielding

$$\begin{pmatrix} \nabla \times E \\ \nabla \times H \end{pmatrix} = J \begin{pmatrix} E \\ H \end{pmatrix}, \quad J := \frac{1}{(1 - \chi^2 k^2)} \begin{pmatrix} \chi k^2 & i\omega\mu \\ -i\omega\epsilon & \chi k^2 \end{pmatrix},$$

where $k^2 = \omega^2 \epsilon\mu$, which we term the *Maxwell–DBF equation*. For obvious reasons we now make the assumption that $(1 - \chi^2 k^2) \neq 0$ which is typically enforced with

$$-1 < \chi k < 1. \tag{2}$$

The permittivity, permeability, and chirality are all taken to be $d_x \times d_y$ bi–periodic

$$\{\epsilon, \mu, \chi\}(x, y, z) = \begin{cases} \{\epsilon^{(u)}, \mu^{(u)}, 0\}, & z > h, \\ \{\epsilon^{(v)}, \mu^{(v)}, \chi^{(v)}\}(x, y, z), & -h < z < h, \\ \{\epsilon^{(w)}, \mu^{(w)}, 0\}, & z < -h, \end{cases}$$

where $\epsilon^{(u)}, \epsilon^{(w)}, \mu^{(u)}, \mu^{(w)} \in \mathbf{R}^+$,

$$\{\epsilon^{(v)}, \mu^{(v)}, \chi^{(v)}\}(x + d_x, y + d_y, z) = \{\epsilon^{(v)}, \mu^{(v)}, \chi^{(v)}\}(x, y, z),$$

and

$$\lim_{z \to h-} \{\epsilon^{(v)}, \mu^{(v)}, \chi^{(v)}\}(x, y, z) = \{\epsilon^{(u)}, \mu^{(u)}, 0\},$$
$$\lim_{z \to (-h)+} \{\epsilon^{(v)}, \mu^{(v)}, \chi^{(v)}\}(x, y, z) = \{\epsilon^{(w)}, \mu^{(w)}, 0\}.$$

For future use $(k^{(m)})^2 = \epsilon^{(m)} \mu^{(m)} \omega^2$, $m \in \{u, v, w\}$.

As in our previous contributions, we consider such structures illuminated from above by plane–wave incident radiation of the form

$$E^{\text{inc}}(x, y, z) = A^E \exp(i\alpha x + i\beta y - i\gamma^{(u)} z),$$
$$H^{\text{inc}}(x, y, z) = A^H \exp(i\alpha x + i\beta y - i\gamma^{(u)} z),$$

where

$$\left|A^E\right| = \left|A^H\right| = 1.$$

In order to solve the governing equations in the achiral ($\chi = 0$) upper layer, $\{z > h\}$, we ask that

$$\underline{k} \times A^E = i\omega\mu^{(u)} A^H, \quad \underline{k} \times A^H = -i\omega\epsilon^{(u)} A^E, \quad \underline{k} \cdot A^E = 0, \quad \underline{k} \cdot A^H = 0,$$

where

$$\underline{k} = \begin{pmatrix} \alpha \\ \beta \\ -\gamma^{(u)} \end{pmatrix} = k^{(u)} \begin{pmatrix} \sin(\theta)\cos(\phi) \\ \sin(\theta)\sin(\phi) \\ \cos(\theta) \end{pmatrix},$$

and (ϕ, θ) are the angles of incidence.

3 Transparent Boundary Conditions

We now give a brief reprise of our description in [47,52,51] of the transparent boundary conditions we enforce. (See also the text of Bao & Li [9].) These allow us to not only reduce the infinite domain to one of finite size, but also rigorously specify far–field boundary conditions. In the upper domain $\{z > h\}$ we seek a solution in the sum of the incident radiation and an upward propagating (reflected) component, e.g.,

$$\begin{aligned} E &= E^{\text{inc}} + E^{\text{refl}} \\ &= A^E \exp(i\alpha x + i\beta y - i\gamma^{(u)} z) + c_{0,0} \exp(i\alpha x + i\beta y + i\gamma^{(u)}(z-h)) \\ &\quad + \sum_{(p,q)\neq(0,0)} \hat{u}_{p,q} \exp(i\alpha_p x + i\beta_q y + i\gamma^{(u)}_{p,q}(z-h)), \end{aligned}$$

[54,67] where

$$\alpha_p = \alpha + (2\pi/d_x)p, \quad \beta_q = \beta + (2\pi/d_y)q,$$

$$\gamma^{(m)}_{p,q} := \begin{cases} \sqrt{(k^{(m)})^2 - \alpha_p^2 - \beta_q^2}, & \alpha_p^2 + \beta_q^2 \le \epsilon^{(m)} k_0^2, \\ i\sqrt{\alpha_p^2 + \beta_q^2 - (k^{(m)})^2}, & \alpha_p^2 + \beta_q^2 > \epsilon^{(m)} k_0^2, \end{cases} \quad m \in \{u, w\},$$

since $\epsilon^{(u)}, \epsilon^{(w)}, \mu^{(u)}, \mu^{(w)} \in \mathbf{R}^+$. By choosing $c_{0,0} = \hat{u}_{0,0} - A^E \exp(-i\gamma^{(u)} h)$, which implies that $\hat{u}_{0,0} = c_{0,0} + A^E \exp(-i\gamma^{(u)} h)$, we have

$$\begin{aligned} E &= A^E \exp(i\alpha x + i\beta y - i\gamma^{(u)} z) - A^E \exp(i\alpha x + i\beta y + i\gamma^{(u)}(z-2h)) \\ &\quad + \sum_{p=-\infty}^{\infty} \sum_{q=-\infty}^{\infty} \hat{u}_{p,q} \exp(i\alpha_p x + i\beta_q y + i\gamma^{(u)}_{p,q}(z-h)), \end{aligned}$$

and $E(x, y, h) = u(x, y)$. Now, one can show that

$$\begin{aligned} \partial_z E &= (-i\gamma^{(u)}) A^E \exp(i\alpha x + i\beta y - i\gamma^{(u)} z) \\ &\quad - (i\gamma^{(u)}) A^E \exp(i\alpha x + i\beta y + i\gamma^{(u)}(z-2h)) \\ &\quad + \sum_{p=-\infty}^{\infty} \sum_{q=-\infty}^{\infty} (i\gamma^{(u)}_{p,q}) \hat{u}_{p,q} \exp(i\alpha_p x + i\beta_q y + i\gamma^{(u)}_{p,q}(z-h)), \end{aligned}$$

so that

$$\begin{aligned} -\partial_z E(x, y, h) &= (i\gamma^{(u)}) A^E \exp(i\alpha x + i\beta y - i\gamma^{(u)} h) \\ &\quad + (i\gamma^{(u)}) A^E \exp(i\alpha x + i\beta y + i\gamma^{(u)}(-h)) \\ &\quad + \sum_{p=-\infty}^{\infty} \sum_{q=-\infty}^{\infty} (-i\gamma^{(u)}_{p,q}) \hat{u}_{p,q} \exp(i\alpha_p x + i\beta_q y). \end{aligned}$$

Defining the function

$$\phi(x, y) := \left(2i\gamma^{(u)} \exp(-i\gamma^{(u)} h)\right) A^E \exp(i\alpha x + i\beta y),$$

and the order–one Fourier multiplier (the externally directed Dirichlet–Neumann operator for the Maxwell equation on $\{z > h\}$)

$$T_u[\psi] := \sum_{p=-\infty}^{\infty} \sum_{q=-\infty}^{\infty} (-i\gamma_{p,q}^{(u)}) \hat{\psi}_{p,q} \exp(i\alpha_p x + i\beta_q y),$$

we see that we can express the Upward Propagating Condition (UPC) [4] exactly with the boundary condition

$$-\partial_z E(x,y,h) - T_u[E(x,y,h)] = \phi(x,y).$$

In an analogous fashion we discover that

$$-\partial_z H(x,y,h) - T_u[H(x,y,h)] = \psi(x,y),$$

where

$$\psi(x,y) := \left(2i\gamma^{(u)} \exp(-i\gamma^{(u)} h)\right) A^H \exp(i\alpha x + i\beta y).$$

Similarly, in $\{z < -h\}$ we seek a solution which is purely downward propagating (transmitted)

$$E = E^{\text{trans}} = \sum_{p=-\infty}^{\infty} \sum_{q=-\infty}^{\infty} \hat{w}_{p,q} \exp(i\alpha_p x + i\beta_q y - i\gamma_{p,q}^{(w)}(z+h)),$$

[54,67]. Clearly $E(x,y,-h) = w(x,y)$ and, using

$$\partial_z E(x,y,-h) = \sum_{p=-\infty}^{\infty} \sum_{q=-\infty}^{\infty} (-i\gamma_{p,q}^{(w)}) \hat{w}_{p,q} \exp(i\alpha_p x + i\beta_q y),$$

we define the analogous order–one Fourier multiplier (again, the externally directed Dirichlet–Neumann operator for the Maxwell equation on $\{z < -h\}$)

$$T_w[\psi] := \sum_{p=-\infty}^{\infty} \sum_{q=-\infty}^{\infty} (-i\gamma_{p,q}^{(w)}) \hat{\psi}_{p,q} \exp(i\alpha_p x + i\beta_q y).$$

We can state the Downward Propagating Condition (DPC) [4] transparently using

$$\partial_z E(x,y,-h) - T_w[E(x,y,-h)] = 0,$$

and

$$\partial_z H(x,y,-h) - T_w[H(x,y,-h)] = 0.$$

Gathering our full set of governing equations we find the following problem to solve,

$$\begin{pmatrix} \nabla \times E \\ \nabla \times H \end{pmatrix} = J \begin{pmatrix} E \\ H \end{pmatrix}, \qquad -h < z < h, \tag{3a}$$

$$-\partial_z E - T_u[E] = \phi, \quad -\partial_z H - T_u[H] = \psi, \qquad z = h, \tag{3b}$$

$$\partial_z E - T_w[E] = 0, \quad \partial_z H - T_w[H] = 0, \qquad z = -h, \tag{3c}$$

$$E(x + d_x, y + d_y, z) = \exp(i\alpha d_x + i\beta d_y) E(x,y,z), \tag{3d}$$

$$H(x + d_x, y + d_y, z) = \exp(i\alpha d_x + i\beta d_y) H(x,y,z). \tag{3e}$$

4 A Chiral Slab in Vacuum

We begin our study by considering a periodic chiral slab in a vacuum where we have constant values of the permittivity and permeability

$$\epsilon^{(m)} = \epsilon_0, \quad \mu^{(m)} = \mu_0, \quad k^{(m)} = k_0 = \sqrt{\epsilon_0 \mu_0}\omega, \quad m \in \{u, w\}.$$

Additionally we choose $\epsilon^{(v)} = \epsilon_0$ and $\mu^{(v)} = \mu_0$ for simplicity, though, any constant value can be accommodated. As we will see, this constant permeability/permittivity assumption enables a change of variables which not only delivers a significantly simpler set of PDEs, but also reveals a particularly insightful physical interpretation.

4.1 Decoupling by Polarization

In this case of *constant* values of the permeability and permittivity, we can decouple the solutions of the Maxwell equations by polarization (left– and right–handed). To demonstrate the decoupling we appeal to the Maxwell–DBF equations in $\{-h < z < h\}$, (3a), in this setting

$$\begin{pmatrix} \nabla \times E \\ \nabla \times H \end{pmatrix} = J_0 \begin{pmatrix} E \\ H \end{pmatrix}, \quad J_0 := \frac{1}{(1 - \chi^2 k_0^2)} \begin{pmatrix} \chi k_0^2 & i\omega\mu_0 \\ -i\omega\epsilon_0 & \chi k_0^2 \end{pmatrix},$$

where we enforce $-1 < \chi k_0 < 1$, c.f. (2). To decouple this system, we compute the eigenvalues and eigenvectors of the matrix J_0, which are readily shown to be

$$\lambda_L = \frac{k_0(\chi k_0 + 1)}{1 - \chi^2 k_0^2} = \left(\frac{k_0}{1 - \chi k_0} \right) =: \kappa^L, \quad \xi^L = \begin{pmatrix} 1 \\ -i/\eta_0 \end{pmatrix},$$

where $\eta_0 = \sqrt{\mu_0/\epsilon_0}$ is the vacuum impedance, and

$$\lambda_R = \frac{k_0(\chi k_0 - 1)}{1 - \chi^2 k_0^2} = -\left(\frac{k_0}{1 + \chi k_0} \right) =: -\kappa^R, \quad \xi^R = \begin{pmatrix} -i\eta_0 \\ 1 \end{pmatrix}.$$

With these we can form the diagonal and diagonalizing matrices

$$\Lambda = \begin{pmatrix} \kappa^L & 0 \\ 0 & -\kappa^R \end{pmatrix}, \quad V_0 = \begin{pmatrix} 1 & -i\eta_0 \\ -i/\eta_0 & 1 \end{pmatrix}, \quad V_0^{-1} = \begin{pmatrix} 1/2 & i\eta_0/2 \\ i/(2\eta_0) & 1/2 \end{pmatrix}.$$

Setting

$$\begin{pmatrix} L \\ R \end{pmatrix} = V_0^{-1} \begin{pmatrix} E \\ H \end{pmatrix} \quad \Longleftrightarrow \quad \begin{pmatrix} E \\ H \end{pmatrix} = V_0 \begin{pmatrix} L \\ R \end{pmatrix}, \tag{4}$$

we have the Bohren Transformation [35, 34]. With these, it is not difficult to show that L and R satisfy,

$$\nabla \times L = \kappa^L L, \quad \nabla \times R = -\kappa^R R, \tag{5}$$

respectively, establishing them as Beltrami Fields [34]. The suggestive notation now becomes clear: The field L is Left Circularly Polarized (LCP) while R is

Right Circularly Polarized (RCP). We notice that this change of variables is independent of the chirality, χ, which could be zero, non–zero, or even non–constant. This gives the classical observation that all solutions of Maxwell's equations in a homogeneous medium are composed of LCP and RCP plane–waves.

In the case of an achiral material, $\chi \equiv 0$, we have that $\kappa^L = \kappa^R = k_0$ and both polarities travel at the *same* speed. However, for chiral materials, $\chi \neq 0$, $\kappa^L \neq \kappa^R$ and the polarizations travel at *different* speeds; this is circular dichromism (CD).

4.2 Transverse Solution: Beltrami Equations

While not immediately apparent, the Beltrami equations, (5), admit transverse solutions in particular configurations. To illustrate this we consider the generic variable (y–invariant) coefficient Beltrami equation

$$\nabla \times Q = \frac{\sigma_0}{\sigma(x,z)} Q,$$

where the particular form will become clear presently, and consider y–invariant solutions of the form

$$Q = Q(x,z) = \begin{pmatrix} q^x(x,z) \\ q(x,z) \\ q^z(x,z) \end{pmatrix}.$$

It is not difficult to see that the Beltrami equation demands

$$\begin{aligned} -\partial_z q(x,z) &= \sigma_0 \left(\frac{q^x(x,z))}{\sigma(x,z)} \right), \\ \partial_z q^x(x,z) - \partial_x q^z(x,z) &= \sigma_0 \left(\frac{q(x,z)}{\sigma(x,z)} \right), \\ \partial_x q(x,z) &= \sigma_0 \left(\frac{q^z(x,z)}{\sigma(x,z)} \right). \end{aligned}$$

The first and third equations can be readily solved in terms of $q(x,z)$,

$$q^x(x,z) = -\frac{\sigma(x,z)\partial_z q(x,z)}{\sigma_0}, \quad q^z(x,z) = \frac{\sigma(x,z)\partial_x q(x,z)}{\sigma_0},$$

and insertion of these into the second equation yields

$$\partial_z \left[-\frac{\sigma(x,z)\partial_z q(x,z)}{\sigma_0} \right] - \partial_x \left[\frac{\sigma(x,z)\partial_x q(x,z)}{\sigma_0} \right] = \sigma_0 \frac{q(x,z)}{\sigma(x,z)},$$

or

$$\sigma(x,z)\mathrm{div}\left[\sigma(x,z)\nabla q(x,z)\right] + \sigma_0^2 q(x,z) = 0. \tag{6}$$

Naturally, if $\sigma \equiv 1$ then we realize a standard Helmholtz equation

$$\Delta q(x,z) + \sigma_0^2 q(x,z) = 0,$$

however, even if $\sigma = \sigma(x,z)$, (6) is a *scalar* PDE of elliptic type for which our techniques are applicable.

4.3 Two–Dimensional Chirality

With these developments, it is easy to see that if the chirality is y–independent, $\chi = \chi(x,z)$, and x–periodic (with period $d_x = d$), then the fields $\{L, R\}$ can be decomposed as

$$L = \begin{pmatrix} \ell^x(x,z) \\ \ell(x,z) \\ \ell^z(x,z) \end{pmatrix}, \quad R = \begin{pmatrix} r^x(x,z) \\ r(x,z) \\ r^z(x,z) \end{pmatrix},$$

with the *transverse* components satisfying the following elliptic PDEs. Using $\sigma_0 = k_0$ and $\sigma(x,z) = 1 - k_0\chi(x,z)$ for the LCP field we find

$$(1 - k_0\chi(x,z))\operatorname{div}\left[(1 - k_0\chi(x,z))\nabla\ell(x,z)\right] + k_0^2\ell(x,z) = 0.$$

Using $\sigma_0 = -k_0$ and $\sigma(x,z) = 1 + k_0\chi(x,z)$ for the RCP field we find

$$(1 + k_0\chi(x,z))\operatorname{div}\left[(1 + k_0\chi(x,z))\nabla r(x,z)\right] + k_0^2 r(x,z) = 0.$$

In this case of transverse polarization we realize that there are two *decoupled* PDEs to solve. The first, using the (inverse) Bohren transformation (4) for the data at Γ_h, is for the LCP field,

$$(1 - k_0\chi^{(v)}(x,z))\operatorname{div}\left[(1 - k_0\chi^{(v)}(x,z))\nabla\ell(x,z)\right] + k_0^2\ell(x,z) = 0, \quad -h < z < h, \tag{7a}$$

$$-\partial_z\ell - T_u[\ell] = \frac{1}{2}(\phi + i\eta_0\psi), \quad z = h, \tag{7b}$$

$$\partial_z\ell - T_w[\ell] = 0, \quad z = -h, \tag{7c}$$

$$\ell(x+d,z) = \exp(i\alpha d)\ell(x,z). \tag{7d}$$

The second, again via the (inverse) Bohren transformation (4) for the condition at Γ_h, is for the RCP field,

$$(1 + k_0\chi^{(v)}(x,z))\operatorname{div}\left[(1 + k_0\chi^{(v)}(x,z))\nabla r(x,z)\right] + k_0^2 r(x,z) = 0, \quad -h < z < h, \tag{8a}$$

$$-\partial_z r - T_u[r] = \frac{1}{2}\left(\frac{i\phi}{\eta_0} + \psi\right), \quad z = h, \tag{8b}$$

$$\partial_z r - T_w[r] = 0, \quad z = -h, \tag{8c}$$

$$r(x+d,z) = \exp(i\alpha d)r(x,z). \tag{8d}$$

To aid future developments we give a unified statement of (7) and (8) as

$$
\begin{aligned}
&\rho(x,z)\mathrm{div}\left[\rho(x,z)\nabla v(x,z)\right] + k_0^2 v(x,z) = 0, && \text{in } S_v, && \text{(9a)}\\
&-\partial_z v - T_u[v] = \tau, && \text{at } \mathit{\Gamma}_h, && \text{(9b)}\\
&\partial_z v - T_w[v] = 0, && \text{at } \mathit{\Gamma}_{-h}, && \text{(9c)}\\
&v(x+d,z) = \exp(i\alpha d) v(x,z). && && \text{(9d)}
\end{aligned}
$$

where

$$
v(x,z) = \begin{cases} \ell(x,z), & \text{LCP}, \\ r(x,z), & \text{RCP}, \end{cases} \quad \rho(x,z) = \begin{cases} 1 - k_0 \chi^{(v)}(x,z), & \text{LCP}, \\ 1 + k_0 \chi^{(v)}(x,z), & \text{RCP}, \end{cases}
$$

and

$$
\tau = \begin{cases} \frac{1}{2}(\phi + i\eta_0 \psi), & \text{LCP}, \\ \frac{1}{2}(\frac{i\phi}{\eta_0} + \psi), & \text{RCP}, \end{cases} \tag{10}
$$

and

$$
S_v := (0,d) \times (-h,h), \quad \mathit{\Gamma}_{\pm h} := (0,d) \times \{z = \pm h\}.
$$

5 A High–Order Perturbation of Envelopes Method

Following the lead of our previous work on the HOPE approach to the achiral Helmholtz and Maxwell equations [47,52,51], we suppose that the chirality is an (initially) small perturbation of a base value, $\bar{\chi}$,

$$
\chi^{(v)}(x,z) = \bar{\chi} - \delta X(x,z),
$$

which has a slightly different form than [47,52,51] in order to accommodate the case that, perhaps, $\bar{\chi} = 0$. This gives

$$
\rho(x,z) = \rho_0 + \delta \rho_1(x,z),
$$

$$
\rho_0 = \begin{cases} 1 - k_0 \bar{\chi}, & \text{LCP}, \\ 1 + k_0 \bar{\chi}, & \text{RCP}, \end{cases} \quad \rho_1(x,z) = \begin{cases} k_0 X(x,z), & \text{LCP}, \\ -k_0 X(x,z), & \text{RCP}, \end{cases}
$$

and, as above, $-1 < \bar{\chi} k_0 < 1$, c.f. (2). With this (9) becomes

$$
\begin{aligned}
&\rho_0 \mathrm{div}\left[\rho_0 \nabla v(x,z)\right] + k_0^2 v(x,z) = F(x,z), && \text{in } S_v, && \text{(11a)}\\
&-\partial_z v - T_u[v] = \tau, && \text{at } \mathit{\Gamma}_h, && \text{(11b)}\\
&\partial_z v - T_w[v] = 0, && \text{at } \mathit{\Gamma}_{-h}, && \text{(11c)}\\
&v(x+d,z) = \exp(i\alpha d) v(x,z), && && \text{(11d)}
\end{aligned}
$$

where

$$
\begin{aligned}
F(x,z) = &-\delta \rho_0 \mathrm{div}\left[\rho_1(x,z) \nabla v(x,z)\right] - \delta \rho_1(x,z) \mathrm{div}\left[\rho_0 \nabla v(x,z)\right] \\
&- \delta^2 \rho_1(x,z) \mathrm{div}\left[\rho_1(x,z) \nabla v(x,z)\right].
\end{aligned} \tag{11e}
$$

We now expand

$$v(x,z;\delta) = \sum_{m=0}^{\infty} v_m(x,z)\delta^m, \tag{12}$$

and insert this into (11) giving the recursive problems for $v_m(x,z)$ as

$$\begin{aligned}
&\rho_0 \mathrm{div}\left[\rho_0 \nabla v_m(x,z)\right] + k_0^2 v_m(x,z) = F_m(x,z), && \text{in } S_v, && \text{(13a)}\\
&-\partial_z v_m - T_u[v_m] = \delta_{m,0}\tau, && \text{at } \Gamma_h, && \text{(13b)}\\
&\partial_z v_m - T_w[v_m] = 0, && \text{at } \Gamma_{-h}, && \text{(13c)}\\
&v_m(x+d,z) = \exp(i\alpha d) v_m(x,z), && && \text{(13d)}
\end{aligned}$$

where, $\delta_{m,n}$ is the Kronecker delta function, and

$$\begin{aligned}
F_m(x,z) = &-\rho_0 \mathrm{div}\left[\rho_1(x,z)\nabla v_{m-1}(x,z)\right] - \rho_1(x,z)\mathrm{div}\left[\rho_0 \nabla v_{m-1}(x,z)\right]\\
&- \rho_1(x,z)\mathrm{div}\left[\rho_1(x,z)\nabla v_{m-2}(x,z)\right]. \qquad \text{(13e)}
\end{aligned}$$

We note that we can solve each of these at order zero with plane wave solutions

$$v_0(x,z) = A\exp(i\alpha x - i\bar{\gamma} z), \quad \alpha^2 + \bar{\gamma}^2 = \frac{k_0^2}{\rho_0^2}.$$

A helpful point of view of our HOPE scheme is that we seek higher order corrections to these solutions

$$v(x,z) = v_0(x,z) + \sum_{m=1}^{\infty} v_m(x,z)\delta^m.$$

To specify more clearly the nature of our algorithm we must clarify the form of the envelope, $X(x,z)$. For the numerical experiments of § 9 we follow the lead of our previous work [47] and choose one meant to emulate a solid layer of chiral material. Consider the smooth bump function

$$\Phi_{a,b}(z) := \frac{\tanh(w(z-a)) - \tanh(w(z-b))}{2},$$

with sharpness parameter w, which is essentially unity on (a,b) while being effectively zero outside. We desire a uniform chiral layer of thickness $2t$ and chirality χ' in an otherwise achiral material by choosing

$$\bar{\chi} = 0, \quad X(x,z) = \chi' \Phi_{-t,t}(z), \quad \delta = -1. \tag{14}$$

In Figure 1 we plot the resulting $\chi^{(v)}(x,z)$ for $d = 0.8$, $h = 0.95$, $t = 0.5$, $\chi' = 0.01$, and $w = 100$.

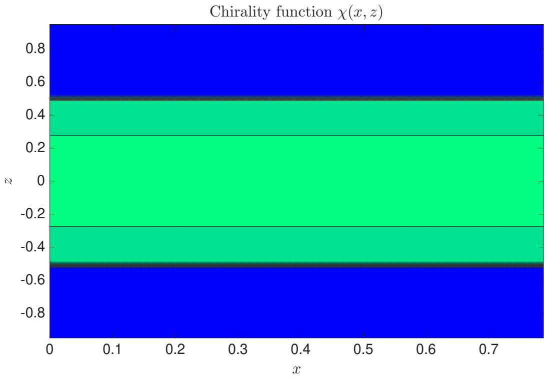

Fig. 1: Plot of an example chirality function, $\chi^{(v)}(x, z)$, approximating a chiral slab of unit thickness.

6 Function Spaces

We now recall function spaces and theoretical results that are necessary for our analysis, very much in the spirit of our previous work [47, 52, 51]. For any real number $s \geq 0$, we have the interfacial quasiperiodic L^2 Sobolev norm

$$\|v\|_{H^s}^2 := \sum_{p=-\infty}^{\infty} \langle p \rangle^{2s} |\hat{v}_p|^2 ,$$

where

$$\langle p \rangle^2 := 1 + |p|^2 , \quad \hat{v}_p := \frac{1}{d} \int_0^d v(x) e^{-i\alpha_p x} \, dx.$$

From this we define the interfacial quasiperiodic Sobolev space [32]

$$H^s(\Gamma) = \left\{ v(x) \in L^2(\Gamma) \mid \|v\|_{H^s} < \infty \right\} , \quad \Gamma := (0, d).$$

In addition, we mention that the dual space of H^s, H^{-s}, can be defined by the norm above with a negative index. We also recall the space of s–times continuously differentiable functions with Hölder norm

$$|g|_{C^s} := \max_{0 \leq \ell + r \leq s} \left| \partial_x^\ell \partial_z^r g(x, z) \right|_{L^\infty} .$$

Finally, we define the volumetric laterally quasiperiodic Sobolev space as

$$H^s(S_v) = \left\{ u(x, z) \in L^2(S_v) \mid \|u\|_{H^s} < \infty \right\} ,$$

where

$$\|u\|_{H^s}^2 := \sum_{j=0}^{s} \sum_{p=-\infty}^{\infty} \langle p \rangle^{2(s-j)} \int_{-h}^{h} \left| \partial_z^j \hat{u}_p(z) \right|^2 \, dz.$$

We mention an important lemma [17, 48] required for our later proofs.

Lemma 61 *Let $s \geq 0$ be an integer and D be either Γ or S_v. If $g \in C^s(D)$ and $w \in H^s(D)$ then $gw \in H^s(D)$ and*

$$\|gw\|_{H^s} \leq \tilde{M}(s, D) \, |g|_{C^s} \, \|w\|_{H^s} \, ,$$

where $\tilde{M}$ is some positive constant.

For our results on joint analyticity we require a particular notion of analytic function.

Definition 62 *Given any integer $\ell \geq 0$, the functions $f = f(x)$ and $X = X(x, z)$ are members of the spaces $C^\omega_\ell(\Gamma)$ and $C^\omega_\ell(S_v)$, respectively, if they are real analytic and satisfy the estimates*

$$\left| \frac{\partial_x^r}{r!} f \right|_{C^\ell} \leq C_f \frac{A^r}{(r+1)^2}, \quad \left| \frac{\partial_x^r \partial_z^t}{(r+t)!} X \right|_{C^\ell} \leq C_X \frac{A^r}{(r+1)^2} \frac{D^t}{(t+1)^2}, \quad \forall \; r, t \geq 0,$$

for some $C_f, C_X, A, D > 0$.

Finally, we recall the following elementary result [49, 47].

Lemma 63 *Let $s \geq 0$ be an integer, then there exists a constant $S > 0$ such that*

$$\sum_{j=0}^{s} \frac{(s+1)^2}{(s-j+1)^2 (j+1)^2} < S, \quad \sum_{j=0}^{s} \sum_{r=0}^{j} \frac{(s+1)^2}{(s-j+1)^2 (j-r+1)^2 (r+1)^2} < S^2.$$

7 Analytic Continuation

As we will demonstrate shortly, in either left or right circular polarization, the series (12) is strongly convergent in an appropriate function space. In theory, this demands that $\delta \ll 1$, which suffices for small deviations of the chirality from its background value, however, with a little more effort we can demonstrate that the field $v(x, z; \delta)$ is, in fact, analytic for *any real* value of the perturbation parameter δ. We follow our previous work [47, 51] (inspired by the proofs which can be found in [49, 50]) and conclude from this result that numerical analytic continuation algorithms, such as Padé approximation [8], are fully justified.

To accomplish this proof, we consider the envelope $X(x, z)$ and an *arbitrary real* $\tilde{\delta} \in \mathbf{R}$, and show that v depends *analytically* upon $\tilde{\delta}$. Considering our current framework we set

$$X_0(x, z) := \tilde{\delta}_0 X(x, z), \quad \delta = \tilde{\delta} - \tilde{\delta}_0,$$

and seek analyticity about $\delta = 0$ for

$$\tilde{\delta} X(x, z) = (\tilde{\delta}_0 + \delta) X(x, z) = X_0(x, z) + \delta X(x, z),$$

see Figure 2. With this, we have

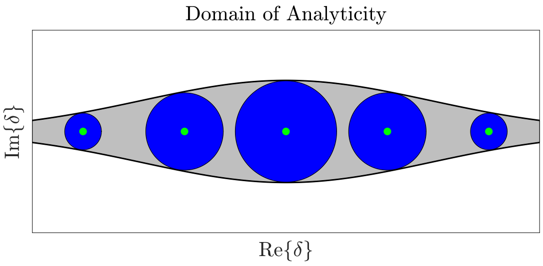

Fig. 2: The domain of analyticity (gray) in the complex plane of the field, (12), as a function of the perturbation parameter, δ. We demonstrate existence of *disks* (blue) of analyticity around arbitrary values $\tilde{\delta}_0 \in \mathbf{R}$ (green) which fills out the entire gray region.

$$\rho(x,z) = \rho_0(x,z) + \delta\rho_1(x,z),$$
$$\rho_0(x,z) = \begin{cases} 1 - k_0\bar{\chi} + k_0 X_0(x,z), \\ 1 + k_0\bar{\chi} - k_0 X_0(x,z), \end{cases} \qquad \rho_1(x,z) = \begin{cases} k_0 X(x,z), & \text{LCP}, \\ -k_0 X(x,z), & \text{RCP}, \end{cases}$$

so that (11) can be updated to

$$\begin{aligned} &\rho_0(x,z)\text{div}\left[\rho_0(x,z)\nabla v(x,z)\right] + k_0^2 v(x,z) = F(x,z), && \text{in } S_v, && \text{(15a)} \\ &-\partial_z v - T_u[v] = \tau, && \text{at } \Gamma_h, && \text{(15b)} \\ &\partial_z v - T_w[v] = 0, && \text{at } \Gamma_{-h}, && \text{(15c)} \\ &v(x+d,z) = \exp(i\alpha d)v(x,z). && && \text{(15d)} \end{aligned}$$

where

$$\begin{aligned} F(x,z) = &-\delta\rho_0(x,z)\text{div}\left[\rho_1(x,z)\nabla v(x,z)\right] \\ &-\delta\rho_1(x,z)\text{div}\left[\rho_0(x,z)\nabla v(x,z)\right] \\ &-\delta^2\rho_1(x,z)\text{div}\left[\rho_1(x,z)\nabla v(x,z)\right]. \end{aligned} \tag{15e}$$

As before, we expand

$$v(x,z;X_0,\delta) = \sum_{m=0}^{\infty} v_m(x,z;X_0)\delta^m, \tag{16}$$

and insert this into (15) giving the recursive problems for $v_m(x,z;X_0)$ as

$$\begin{aligned} &\rho_0(x,z)\text{div}\left[\rho_0(x,z)\nabla v_m(x,z)\right] + k_0^2 v_m(x,z) = F_m(x,z), && \text{in } S_v, && \text{(17a)} \\ &-\partial_z v_m - T_u[v_m] = \delta_{m,0}\tau, && \text{at } \Gamma_h, && \text{(17b)} \\ &\partial_z v_m - T_w[v_m] = 0, && \text{at } \Gamma_{-h}, && \text{(17c)} \\ &v_m(x+d,z) = \exp(i\alpha d)v_m(x,z), && && \text{(17d)} \end{aligned}$$

where

$$\begin{aligned}F_m(x,z) = &-\rho_0(x,z)\mathrm{div}\left[\rho_1(x,z)\nabla v_{m-1}(x,z)\right] \\ &-\rho_1(x,z)\mathrm{div}\left[\rho_0(x,z)\nabla v_{m-1}(x,z)\right] \\ &-\rho_1(x,z)\mathrm{div}\left[\rho_1(x,z)\nabla v_{m-2}(x,z)\right]. \end{aligned} \tag{17e}$$

As in [47] we require an elliptic estimate for our inductive proof which we report here. As [9] states, the issue of *uniqueness* of solutions to the homogeneous Maxwell problem

$$\rho_0(x,z)\mathrm{div}\left[\rho_0(x,z)\nabla V\right] + k_0^2 V = 0, \quad \text{in } S_v, \tag{18a}$$
$$-\partial_z V - T_u[V] = 0, \quad \text{at } \Gamma_h, \tag{18b}$$
$$\partial_z V - T_w[V] = 0, \quad \text{at } \Gamma_{-h}, \tag{18c}$$
$$V(x+d,z) = \exp(i\alpha d)V(x,z), \tag{18d}$$

c.f. (17), which should have only the *trivial* solution $V \equiv 0$, is a difficult one and certain frequencies ω will induce non–uniqueness in some configurations. For better or worse, a precise characterization of the set of forbidden frequencies is unknown and all that is clear is that it is countable and accumulates at infinity [9]. To accommodate this state of affairs we define the set of permissible configurations

$$\mathcal{P} := \left\{(\omega,\bar{\chi},X_0) \mid V \equiv 0 \text{ is the unique solution of (18)}\right\}.$$

With this, we can now state the following fundamental elliptic regularity result.

Theorem 71 *Given any integer $s \geq 0$, if $(\omega,\bar{\chi},X_0) \in \mathcal{P}$, $\rho_0 \in C^{s+1}(S_v)$, $F \in H^s(S_v)$, $Q \in H^{s+1/2}(\Gamma)$, and $R \in H^{s+1/2}(\Gamma)$, then there exists a unique solution of*

$$\begin{aligned}&\rho_0(x,z)\,div\left[\rho_0(x,z)\nabla v\right] + k_0^2 v = F, && in\ S_v,\\ &-\partial_z v - T_u[v] = Q && at\ \Gamma_h,\\ &\partial_z v - T_w[v] = R && at\ \Gamma_{-h},\\ &v(x+d,z) = e^{i\alpha d}v(x,z),\end{aligned}$$

satisfying

$$\|v\|_{H^{s+2}} \leq C_e\left(\|F\|_{H^s} + \|Q\|_{H^{s+1/2}} + \|R\|_{H^{s+1/2}}\right),$$

where $C_e > 0$ is a constant.

Proof This result is very much in the spirit of Theorem 6.2 in [47], both of which can be established using the methods found in [9].

We can now establish the recursive estimate required by our theory.

Lemma 72 *Given any integer $s \geq 0$, if $\rho_0(x,z), \rho_1(x,z) \in C^{s+1}(S_v)$ and*

$$\|v_m\|_{H^{s+2}} \leq KB^m, \quad m < M,$$

then, for the functions F_m in (17e),

$$\|F_M\|_{H^s} \leq K\tilde{M}^2 \left\{ 2\,|\rho_0|_{C^{s+1}}\,|\rho_1|_{C^{s+1}}\,B^{M-1} + |\rho_1|^2_{C^{s+1}}\,B^{M-2} \right\}.$$

Proof We begin our estimations with

$$\|F_M\|_{H^s} \leq \tilde{M}\,|\rho_0|_{C^s}\,\|\rho_1 \nabla v_{M-1}\|_{H^{s+1}} + \tilde{M}\,|\rho_1|_{C^s}\,\|\rho_0 \nabla v_{M-1}\|_{H^{s+1}} \\ + \tilde{M}\,|\rho_1|_{C^s}\,\|\rho_1 \nabla v_{M-2}\|_{H^{s+1}}.$$

Continuing

$$\|F_M\|_{H^s} \leq \tilde{M}\,|\rho_0|_{C^s}\,\tilde{M}\,|\rho_1|_{C^{s+1}}\,\|v_{M-1}\|_{H^{s+2}} + \tilde{M}\,|\rho_1|_{C^s}\,\tilde{M}\,|\rho_0|_{C^{s+1}}\,\|v_{M-1}\|_{H^{s+2}} \\ + \tilde{M}\,|\rho_1|_{C^s}\,\tilde{M}\,|\rho_1|_{C^{s+1}}\,\|v_{M-2}\|_{H^{s+2}}.$$

Finally, the inductive hypothesis yields

$$\|F_M\|_{H^s} \leq 2\tilde{M}^2\,|\rho_0|_{C^{s+1}}\,|\rho_1|_{C^{s+1}}\,KB^{M-1} + \tilde{M}^2\,|\rho_1|^2_{C^{s+1}}\,KB^{M-2},$$

and we are done.

We can now prove our analytic continuation result.

Theorem 73 *Given any integer $s \geq 0$, if $(\omega, \bar{\chi}, X_0) \in \mathcal{P}$, and $\rho_0(x,z), \rho_1(x,z) \in C^{s+1}(S_v)$ then the series* (16) *converges strongly. More precisely,*

$$\|v_m\|_{H^{s+2}} \leq KB^m, \quad \forall\ m \geq 0, \tag{19}$$

for some constants $K, B > 0$.

Proof We prove the estimate (19) by induction. From the definitions of ϕ and ψ it is clear that $\tau \in H^{s+1/2}$ for any $s \geq 0$. For $m = 0$ we invoke Theorem 71 with $F \equiv 0$, $Q = \tau$, and $R \equiv 0$ and set $K := \|v_0\|_{H^{s+2}}$. We now assume that (19) is true for all $m < M$ and use Theorem 71 with $Q \equiv R \equiv 0$ to deduce that

$$\|v_M\|_{H^{s+2}} \leq C_e\,\|F_M\|_{H^s}.$$

From Lemma 72 we have that

$$\|v_M\|_{H^{s+2}} \leq C_e K\tilde{M}^2 \left\{ 2\,|\rho_0|_{C^{s+1}}\,|\rho_1|_{C^{s+1}}\,B^{M-1} + |\rho_1|^2_{C^{s+1}}\,B^{M-2} \right\},$$

and we are done provided that

$$B \geq \max\left\{ 4C_e\tilde{M}^2\,|\rho_0|_{C^{s+1}},\, \sqrt{2C_e}\tilde{M} \right\} |\rho_1|_{C^{s+1}}.$$

Remark 74 *We point out that by setting $X_0 \equiv 0$ we obtain the classical analyticity result about $\tilde{\delta} = 0$.*

Remark 75 *We observe that the choice of B determines the radius of convergence of the series* (16)*, for instance, if we choose $B\delta \leq 1/2$ (implying $\delta \leq 1/(2B)$) then we can guarantee, from* (16)*, that $\|v\|_{H^{s+2}} < 2K$. The dependence of the crucial constant B upon C_e and $|\rho_0|_{C^{s+1}}$, recalling*

$$\rho_0(x,z) = \begin{cases} 1 - k_0\bar{\chi} + k_0 X_0(x,z), & LCP, \\ 1 + k_0\bar{\chi} - k_0 X_0(x,z), & RCP, \end{cases}$$

is somewhat complicated, however, the role of $\tilde{M}\, |\rho_1|_{C^{s+1}}$, remembering

$$\rho_1(x,z) = \begin{cases} k_0 X(x,z), & LCP, \\ -k_0 X(x,z), & RCP, \end{cases}$$

is clear: Linear dependence upon $\tilde{M}$ and $|\rho_1|_{C^{s+1}} = k_0\, |X(x,z)|_{C^{s+1}}$.

8 Joint Analyticity

We conclude our theory with a joint analyticity result in the spirit of that found in [47,52] which demonstrates the *joint* analyticity of $v = v(x,z;\delta)$ with respect to x, z, and δ. We accomplish this by showing that the $v_m(x,z)$ from (16) satisfy Definition 62 which is achieved by repeatedly differentiating the problem (17) with respect to x and z.

This requires the generalization of our elliptic estimate, Theorem 71, to the following result.

Theorem 81 *Given any integer $\ell \geq 1$, if $(\omega, \bar{\chi}, X_0) \in \mathcal{P}$, $\rho_0 \in C^{\omega}_{\ell}(S_v)$, so that*

$$\left| \frac{\partial_x^r \partial_z^t}{(r+t)!} \rho_0 \right|_{C^\ell} \leq C_\rho \frac{A^r}{(r+1)^2} \frac{D^t}{(t+1)^2}, \quad \forall\, r,t \geq 0,$$

and some $C_\rho, A, D > 0$, and $F \in C^{\omega}(S_v)$ satisfying

$$\left\| \frac{\partial_x^r \partial_z^t}{(r+t)!} F \right\|_{H^0} \leq C_F \frac{A^r}{(r+1)^2} \frac{D^t}{(t+1)^2}, \quad \forall\, r,t \geq 0,$$

and some $C_F > 0$, and $Q \in C^{\omega}(\Gamma_h)$, $R \in C^{\omega}(\Gamma_{-h})$ satisfying

$$\left\| \frac{\partial_x^r}{r!} Q \right\|_{H^{1/2}} \leq C_Q \frac{A^r}{(r+1)^2}, \quad \left\| \frac{\partial_x^r}{r!} R \right\|_{H^{1/2}} \leq C_R \frac{A^r}{(r+1)^2}, \quad \forall\, r \geq 0,$$

for some $C_Q, C_R > 0$, then there exists a unique solution $V \in C^{\omega}(S_v)$ of

$$\begin{aligned} &\rho_0(x,z)\, div\, [\rho_0(x,z)\nabla V] + k_0^2 V = F, && \text{in } S_v, \\ &-\partial_z V - T_u[V] = Q && \text{at } \Gamma_h, \\ &\partial_z V - T_w[V] = R && \text{at } \Gamma_{-h}, \\ &V(x+d,z) = e^{i\alpha d} V(x,z), \end{aligned}$$

satisfying

$$\left\| \frac{\partial_x^r \partial_z^t}{(r+t)!} V \right\|_{H^2} \leq \underline{C}_e \frac{A^r}{(r+1)^2} \frac{D^t}{(t+1)^2}, \quad \forall\ r,t \geq 0,$$

where

$$\underline{C}_e := \kappa(h)(C_F + C_Q + C_R),$$

for some constant $\kappa(h) > 0$.

Proof The proof of this theorem is similar to that of Theorem 7.2 found in [47].

We now establish a requisite recursive estimate.

Lemma 82 *Given any integer* $\ell \geq 1$*, if* $\rho_0(x,z), \rho_1(x,z) \in C_\ell^\omega(S_v)$ *so that*

$$\left| \frac{\partial_x^r \partial_z^t}{(r+t)!} \rho_0 \right|_{C^\ell} \leq C_\rho \frac{A^r}{(r+1)^2} \frac{D^t}{(t+1)^2}, \quad \left| \frac{\partial_x^r \partial_z^t}{(r+t)!} \rho_1 \right|_{C^\ell} \leq C_\rho \frac{A^r}{(r+1)^2} \frac{D^t}{(t+1)^2},$$

for all $r,t \geq 0$*, for some* $C_\rho, A, D > 0$*, and*

$$\left\| \frac{\partial_x^r \partial_z^t}{(r+t)!} v_m \right\|_{H^2} \leq \underline{K} B^m \frac{A^r}{(r+1)^2} \frac{D^t}{(t+1)^2}, \quad \forall\ m < M, \quad \forall\ r,t \geq 0,$$

for some $\underline{K}, B > 0$ *then for the function* F_M *in* (17e),

$$\left\| \frac{\partial_x^r \partial_z^t}{(r+t)!} F_M \right\|_{H^0} \leq \underline{\tilde{C}K} B^{M-1} \frac{A^r}{(r+1)^2} \frac{D^t}{(t+1)^2},$$

for some $\underline{\tilde{C}} > 0$.

Proof We recall that

$$F_M = -\rho_0 \mathrm{div}\left[\rho_1 \nabla v_{M-1}\right] - \rho_1 \mathrm{div}\left[\rho_0 \nabla v_{M-1}\right] - \rho_1 \mathrm{div}\left[\rho_1 \nabla v_{M-2}\right],$$

and focus on the first term (as the others are similar),

$$F_M^{(1)} = -\rho_0 \mathrm{div}\left[\rho_1 \nabla v_{M-1}\right],$$

so that

$$\begin{aligned} \frac{\partial_x^r \partial_z^t}{(r+t)!} F_M^{(1)} = &-\frac{r!t!}{(r+t)!} \sum_{j=0}^{r} \sum_{k=0}^{j} \sum_{p=0}^{t} \sum_{q=0}^{p} \left(\frac{\partial_x^{r-j}}{(r-j)!} \frac{\partial_z^{t-p}}{(t-p)!} \rho_0 \right) \\ &\times \mathrm{div}\left[\left(\frac{\partial_x^{j-k}}{(j-k)!} \frac{\partial_z^{p-q}}{(p-q)!} \rho_1 \right) \nabla \left\{ \frac{\partial_x^k}{k!} \frac{\partial_z^q}{q!} v_{M-1} \right\} \right]. \end{aligned}$$

Now, using $(r!t!) \leq (r+t)!$, we estimate

$$\begin{aligned}\left\| \frac{\partial_x^r \partial_z^t}{(r+t)!} F_M^{(1)} \right\|_{H^0} &\leq \frac{r!t!}{(r+t)!} \sum_{j=0}^{r} \sum_{k=0}^{j} \sum_{p=0}^{t} \sum_{q=0}^{p} \tilde{M} \left| \frac{\partial_x^{r-j}}{(r-j)!} \frac{\partial_z^{t-p}}{(t-p)!} \rho_0 \right|_{C^0} \\ &\quad \times \tilde{M} \left| \frac{\partial_x^{j-k}}{(j-k)!} \frac{\partial_z^{p-q}}{(p-q)!} \rho_1 \right|_{C^1} \left\| \frac{\partial_x^k}{k!} \frac{\partial_z^q}{q!} v_{M-1} \right\|_{H^2} \\ &\leq \sum_{j=0}^{r} \sum_{k=0}^{j} \sum_{p=0}^{t} \sum_{q=0}^{p} \tilde{M} C_\rho \frac{A^{r-j}}{(r-j+1)^2} \frac{D^{t-p}}{(t-p+1)^2} \\ &\quad \times \tilde{M} C_\rho \frac{A^{j-k}}{(j-k+1)^2} \frac{D^{p-q}}{(p-q+1)^2} \underline{K} B^{M-1} \frac{A^k}{(k+1)^2} \frac{D^q}{(q+1)^2}.\end{aligned}$$

Continuing

$$\begin{aligned}\left\| \frac{\partial_x^r \partial_z^t}{(r+t)!} F_M^{(1)} \right\|_{H^0} &\leq \tilde{M}^2 C_\rho^2 \underline{K} B^{M-1} \frac{A^r}{(r+1)^2} \frac{D^t}{(t+1)^2} \\ &\quad \times \sum_{j=0}^{r} \sum_{k=0}^{j} \frac{(r+1)^2}{(r-j+1)^2 (j-k+1)^2 (k+1)^2} \\ &\quad \times \sum_{p=0}^{t} \sum_{q=0}^{p} \frac{(t+1)^2}{(t-p+1)^2 (p-q+1)^2 (q+1)^2} \\ &\leq \tilde{M}^2 C_\rho^2 \underline{K} B^{M-1} \frac{A^r}{(r+1)^2} \frac{D^t}{(t+1)^2} S^2 S^2,\end{aligned}$$

and we are done provided that we choose

$$\underline{\tilde{C}} \geq \tilde{M}^2 C_\rho^2 S^4.$$

We are now ready to state and establish our joint analyticity result.

Theorem 83 *Given any integer $\ell \geq 1$, if $(\omega, \bar{\chi}, \rho_0) \in \mathcal{P}$, and $\rho_0(x,z), \rho_1(x,z) \in C_\ell^\omega(S_v)$ so that*

$$\left| \frac{\partial_x^r \partial_z^t}{(r+t)!} \rho_0 \right|_{C^\ell} \leq C_\rho \frac{A^r}{(r+1)^2} \frac{D^t}{(t+1)^2}, \quad \left| \frac{\partial_x^r \partial_z^t}{(r+t)!} \rho_1 \right|_{C^\ell} \leq C_\rho \frac{A^r}{(r+1)^2} \frac{D^t}{(t+1)^2},$$

for all $r, t \geq 0$, for some $C_\rho, A, D > 0$, then the series (16) converges strongly. More precisely,

$$\left\| \frac{\partial_x^r \partial_z^t}{(r+t)!} v_m \right\|_{H^2} \leq \underline{K} B^m, \quad \forall\ m, r, t \geq 0, \tag{20}$$

for some constants $\underline{K}, B > 0$.

Proof As before, we prove the estimate (20) by induction. Once again, from the definitions of ϕ and ψ it is clear that $\tau \in C_\ell^\omega$ for some $C_\tau > 0$. For $m = 0$ we invoke Theorem 81 with $F \equiv 0$, $Q = \tau$, and $R \equiv 0$ to realize

$$\left\| \frac{\partial_x^r \partial_z^t}{(r+t)!} v_0 \right\|_{H^2} \leq \kappa(h) C_\tau \frac{A^r}{(r+1)^2} \frac{D^t}{(t+1)^2}, \quad \forall\, r, t \geq 0,$$

and we set $\underline{K} := \kappa(h) C_\tau$. We now assume that (20) is true for all $m < M$ and use Lemma 82 to invoke Theorem 81 with

$$C_F := \underline{\tilde{C} K} B^{M-1}, \quad C_Q = C_R = 0.$$

Therefore we have

$$\left\| \frac{\partial_x^r \partial_z^t}{(r+t)!} \right\|_{H^2} \leq \kappa(h) \underline{\tilde{C} K} B^{M-1} \frac{A^r}{(r+1)^2} \frac{D^t}{(t+1)^2}, \quad \forall\, r, t \geq 0.$$

We are finished provided that we choose

$$B > \kappa(h) \underline{\tilde{C}}.$$

9 Numerical Results

At this point we discuss how a numerical implementation of the HOPE recursions we have derived can be utilized to deliver highly accurate approximations of scattering returns in a robust and reliable manner. We begin with a brief description of our High–Order Spectral (HOS) approach, and then move to comparisons of our approximations to both the exact solution of triply layered media scattering and a smoothed version of this.

9.1 Implementation

The implementation we describe focuses on approximating the solution of (13) in both LCP and RCP cases. Of course this cannot be achieved for *all* $0 \leq m < \infty$ and we naturally approximate solutions with the finite–order truncation of (12),

$$v^M(x, z; \delta) := \sum_{m=0}^{M} v_m(x, z) \delta^m, \tag{21}$$

where the $v_m(x, z)$ approximately satisfy (13) for $0 \leq m \leq M$. For this we appeal to the highly accurate family of HOS methods [21,12,59], in particular, a Fourier–Chebyshev approach. More specifically, we consider

$$v_m(x, z) \approx v_m^{N_x, N_z}(x, z) := \sum_{p=-N_x/2}^{N_x/2-1} \sum_{q=0}^{N_z} \hat{v}_{m,p,q} T_q(z/h) e^{i \alpha_p x},$$

where T_q is the q–th Chebyshev polynomial. To prescribe the Fourier–Chebyshev coefficients, $\{\hat{v}_{m,p,q}\}$, we follow the collocation philosophy by demanding that (13) be true at the gridpoints

$$\{x_j = j(d/N_x) \mid 0 \leq j \leq N_x - 1\}, \quad \{z_r = h\cos(\pi r/N_z) \mid 0 \leq r \leq N_z\}.$$

These constraints generate a sequence of linear systems of equations (at each wavenumber p and order m) which can be rapidly formed via the fast Fourier and Chebyshev transforms [21,12,59], and quickly solved using Gaussian elimination [47].

As with all HOPE algorithms, careful thought is required for the summation which appears in (21). For instance, one must form the sum

$$S^M(\delta) = S^M_{p,q}(\delta) := \sum_{m=0}^{M} \hat{v}_{m,p,q}\delta^m,$$

which approximates the infinite Taylor sum

$$S(\delta) = \sum_{m=0}^{\infty} \hat{v}_{m,p,q}\delta^m.$$

As justified by Theorem 73, this Taylor sum, $S(\delta)$, will converge for all δ in a (perhaps small) neighborhood of the origin in the complex plane. However, Theorem 73 also concludes that the domain of analyticity of $S(\delta)$ includes a (perhaps smaller) neighborhood of the *entire* real axis. A fast and robust algorithm for accessing this region of extended analyticity is Padé approximation [8] which we have used with great success in the past [49,47,52,51]. The Padé approximant of $S^M(\delta)$ is the rational function

$$[P/Q](\delta) := \frac{a^P(\delta)}{b^Q(\delta)} = \frac{\sum_{p=0}^{P} a_p\delta^p}{\sum_{q=0}^{Q} b_q\delta^q},$$

where

$$[P/Q](\delta) = S^M(\delta) + \mathcal{O}(\delta^{P+Q+1}).$$

Well–known formulas exist for the recovery of these $\{a_p, b_q\}$ [8] and the resulting approximants often deliver remarkably accurate approximations of $S(\delta)$, even well outside of the *disk* of convergence of the original Taylor series (see, e.g., Chapter 8 of [10]).

9.2 Scattering by Triply Layered Media

In order to demonstrate the utility of our numerical implementation of the HOPE recursions, we consider a specific problem featuring an exact solution: Scattering of plane electromagnetic radiation by a layered medium featuring achiral and chiral materials with flat interfaces. In more detail, we consider a material with constant permittivity, ϵ_0, and permeability, μ_0, and layered chirality

$$\chi = \chi(z) = \begin{cases} 0, & t < z < h, \\ \chi', & -t < z < t, \\ 0, & -h < z < -t, \end{cases} \tag{22}$$

for $0 < t < h$, with incident radiation τ, (10). It is not difficult to show that the solution of this problem is

$$v(x,z) = \begin{cases} R\exp(i\alpha x + i\gamma z), & t < z < h, \\ U\exp(i\alpha x + i\gamma' z) + D\exp(i\alpha x - i\gamma' z), & -t < z < t, \\ T\exp(i\alpha x - i\gamma z), & -h < z < -t, \end{cases} \tag{23}$$

where

$$\alpha^2 + \gamma^2 = k_0^2, \quad \alpha^2 + (\gamma')^2 = \begin{cases} k_0^2/(1 - k_0\chi')^2, & \text{LCP}, \\ k_0^2/(1 + k_0\chi')^2, & \text{RCP}, \end{cases}$$

and jump conditions at the interfaces deliver a *linear* system of four equations for the four unknowns, $\{R, U, D, T\}$ [67]. These can be readily solved by Gaussian elimination, and we use these as a convenient *exact* solution against which to test our implementation.

Our theorems in their current form do not permit such an irregular chirality function (merely L^∞), but, while such a theory could perhaps be discovered, the resulting numerics would certainly be of very low quality. To avoid this in our numerics we approximate the layered chirality (22) by the smoothed one defined in (14) (see Figure 1) with the choice $w = 100$. With this in hand we can be more precise about our experiments: We selected the following particular geometric constants

$$d = 0.8, \quad h = 0.95, \quad t = 0.5,$$

and electromagnetic constants

$$\lambda = 0.7, \quad \theta = 30^\circ.$$

Akin to [47] we chose two configurations: (i.) small ($\chi' = 0.01$) and (ii.) large ($\chi' = 0.04$) deviations from the zero background chirality. For the small deviation we chose

$$16 \leq N_x \leq 32, \quad 2 \leq M \leq 16,$$

and for the large perturbation case

$$16 \leq N_x \leq 64, \quad 2 \leq M \leq 32,$$

where $N_z = N_x$. We measured errors in the L^∞ norm as

$$\text{Error} = \text{Error}^{N_x,N_z,M} := \left| v^{N_x,N_z,M} - v^{\text{Exact}} \right|_{L^\infty}.$$

9.3 Convergence

We now present the results of our numerical experiments comparing numerical solution of the HOPE recursions versus the flat–interface exact solution. We begin with the small deviation case where $\chi' = 0.01$ and show the convergence of our scheme as $N_x = N_z$ (Figures 3 and 4) and M (Figures 5 and 6) are refined. In a manner similar to our previous work [47], the results are satisfying in that the error appears to decay as the appropriate parameters are increased, however, they are also disappointing as the *spectral* nature of our HOPE method with respect to both the spatial (x and z) and deformation (δ) parameters would suggest an *exponential* rate of convergence [21, 12, 59]. However, this mystery is quickly resolved by noting that solutions in both LCP and RCP will be merely H^1 in the case where $\chi^{(v)} \in L^\infty$. In the next section we return to this issue.

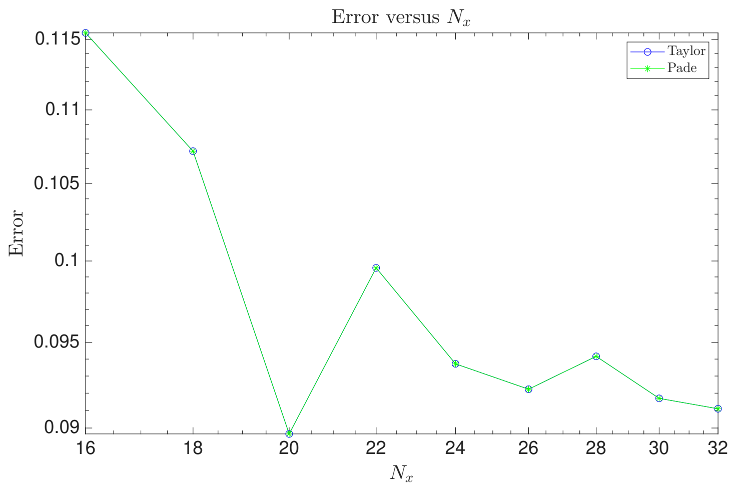

Fig. 3: Error versus N_x for $\chi' = 0.01$ compared with the exact solution: LCP.

We repeated the above experiments in the case of a large deviation $\chi' = 0.04$ and report the results of this in Figures 7, 8, 9, and 10 for $N_x = N_z$ and M refinement, respectively. Here we notice a new phenomena: Substantial divergence of behavior based upon summation method. More specifically, while Padé summation delivers reasonable (though not outstanding) results, Taylor summation produces completely unreliable answers. The reason for this is that for this choice of χ', the value $\delta = -1$ is *outside* the disk of convergence of our solution (12) and only with numerical analytic continuation can we recover useful answers. However, even in the Padé case, we are disappointed with the *rate* of refinement which, as before, is readily explained by the lack of smoothness in the underlying exact solution.

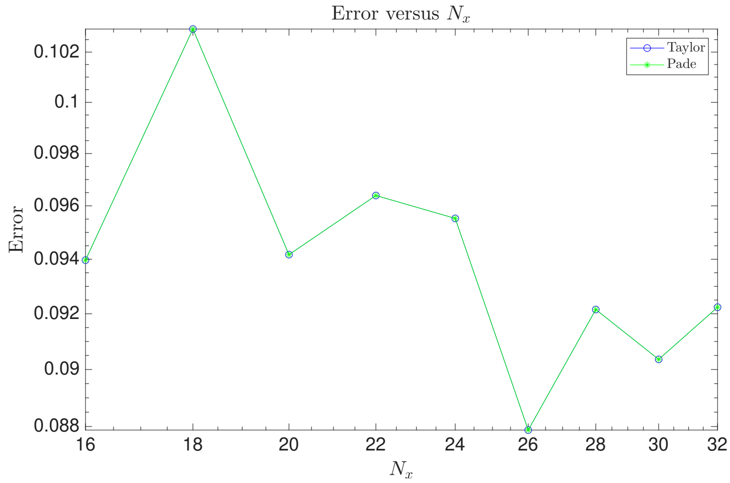

Fig. 4: Error versus N_x for $\chi' = 0.01$ compared with the exact solution: RCP.

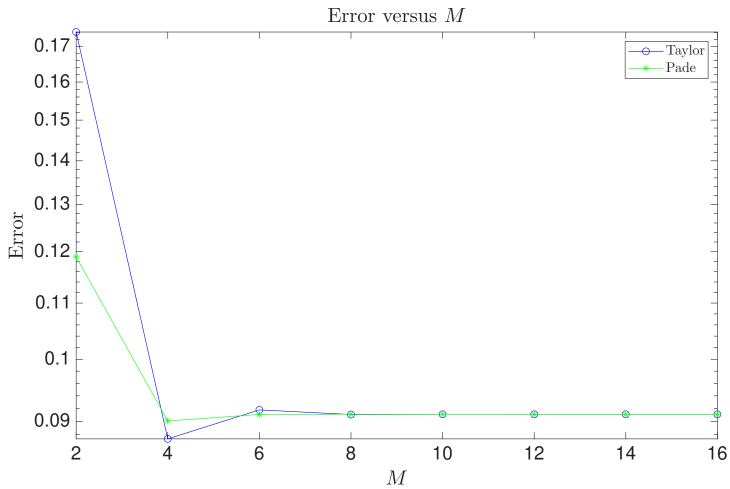

Fig. 5: Error versus M for $\chi' = 0.01$ compared with the exact solution: LCP.

9.4 Convergence to a Smoothed Solution

As we mentioned above, our results thus far have been somewhat disappointing in light of the spectral rate of convergence we were anticipating. To address this concern we repeated these experiments where the exact solution is replaced by a "smoothed" one. For this we took advantage of the fact that if ρ is independent of x then the solution of (9) can be expanded in a (generalized)

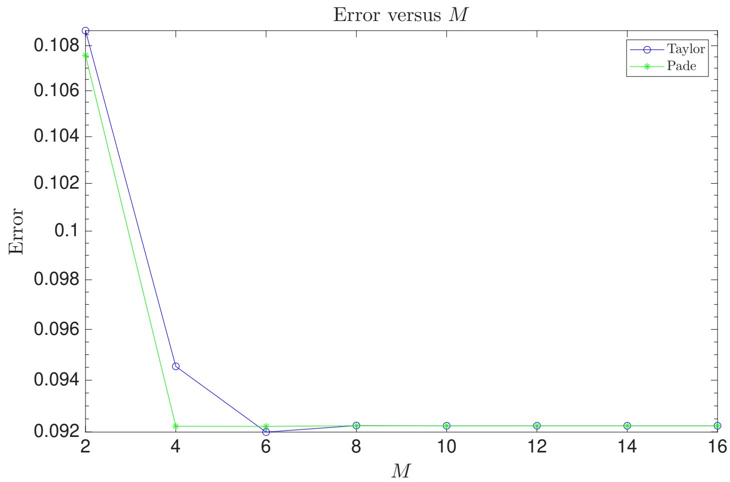

Fig. 6: Error versus M for $\chi' = 0.01$ compared with the exact solution: RCP.

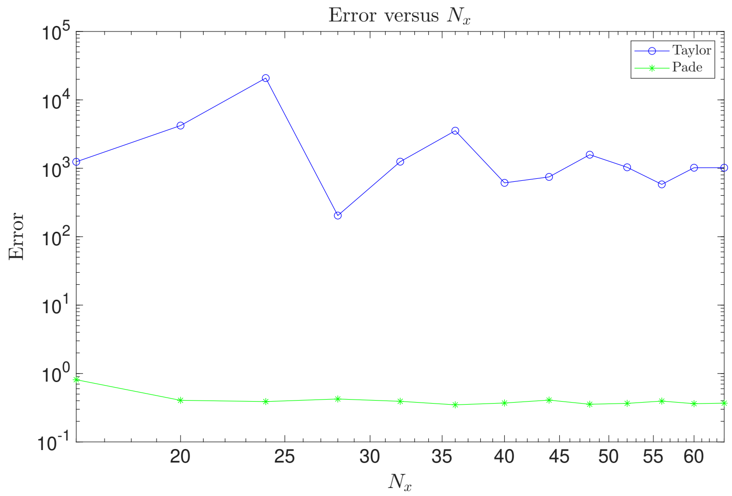

Fig. 7: Error versus N_x for $\chi' = 0.04$ compared with the exact solution: LCP.

Fourier series as

$$v(x, z) = \sum_{p=-\infty}^{\infty} \hat{v}_p(z) e^{i\alpha_p x},$$

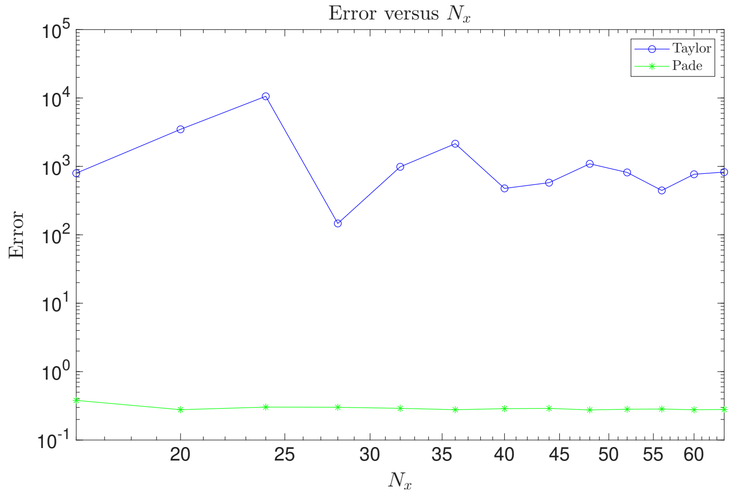

Fig. 8: Error versus N_x for $\chi' = 0.04$ compared with the exact solution: RCP.

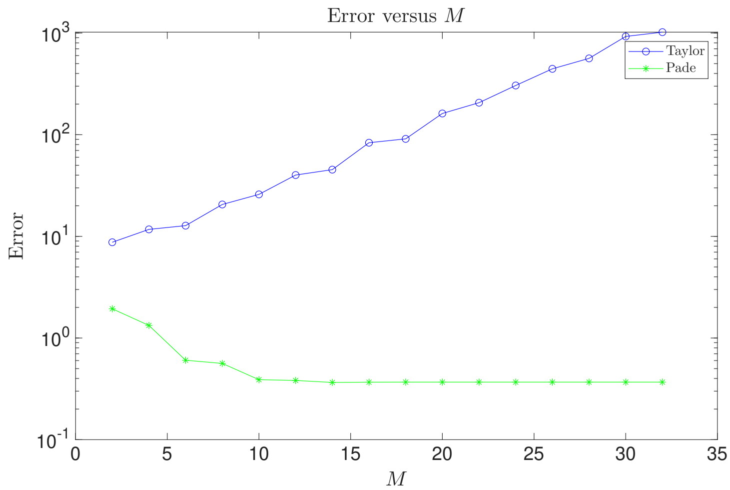

Fig. 9: Error versus M for $\chi' = 0.04$ compared with the exact solution: LCP.

where the resulting $\hat{v}_p(z)$ satisfy

$$\rho(z)\partial_z\left[\rho(z)\partial_z\hat{v}_p(z)\right] + (k_0^2 - \rho(z)^2\alpha_p^2)\hat{v}_p(z) = 0, \qquad -h < z < h, \tag{24a}$$
$$-\partial_z\hat{v}_p - (-i\gamma_p^{(u)})\hat{v}_p = \hat{\tau}_p, \qquad z = h, \tag{24b}$$
$$\partial_z\hat{v}_p - (-i\gamma_p^{(w)})\hat{v}_p = 0, \qquad z = -h, \tag{24c}$$

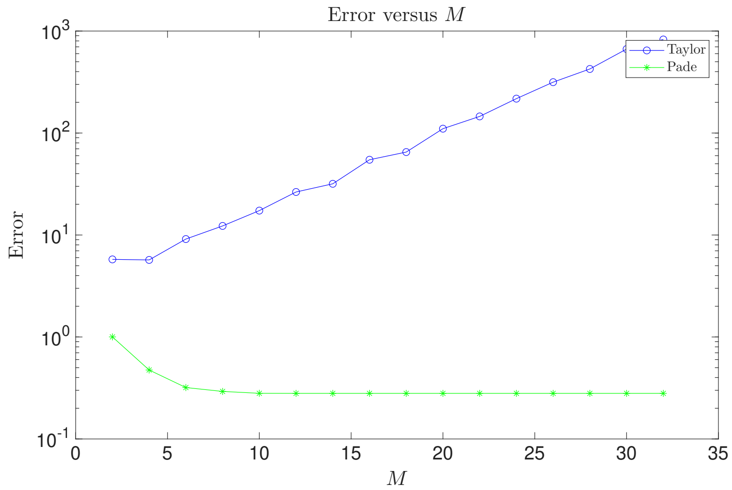

Fig. 10: Error versus M for $\chi' = 0.04$ compared with the exact solution: RCP.

and

$$\hat{\tau}_p = \frac{1}{d} \int_0^d \tau(x) e^{-i\alpha_p x} \, dx,$$

is the p–th Fourier coefficient of $\tau(x)$ [67]. If $\rho(z)$ is piecewise constant then one can express the solution in each homogeneous layer as upward– and downward–propagating modes, c.f. (23), and jump conditions at the interfaces give rise to the readily solved Fresnel equations. To avoid the low regularity of the resulting solutions, we followed our HOPE approach and *approximated* the piecewise constant chirality by the smoothed form (14). While this yields a much smoother approximate solution, one must utilize a numerical algorithm to solve (24). For this we selected the Chebyshev method [21, 12, 59] using the same number of Chebyshev coefficients, specified by N_z, as the relevant HOPE simulation.

We revisited our earlier simulations and report in Figures 11, 12, 13, and 14 results of $N_x = N_z$ and M refinement, respectively, in the small deviation case $\chi' = 0.01$. Now we notice on these log–linear plots the exponential rates of convergence we were hoping to observe. We also notice an enhanced rate of convergence with Padé approximation, even within the disk of convergence which has been observed in the past.

We close with the large deviation case, $\chi' = 0.04$, and plot the outcomes of our simulations in Figures 15, 16, 17, and 18 for increasing $N_x = N_z$ and M, respectively. As $\chi' = 0.04$ pushes the value $\delta = -1$ outside the disk of analyticity of (12) we cannot expect reliable results from Taylor summation (which we observe), however, Padé summation delivers highly resolved answers in a rapid and robust fashion.

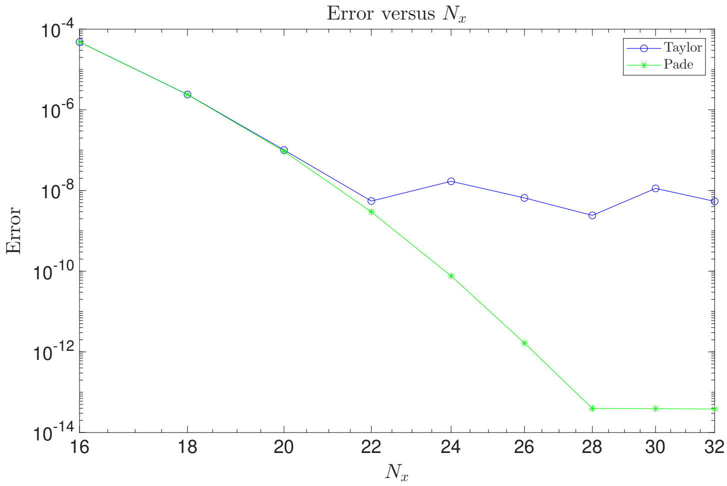

Fig. 11: Error versus N_x for $\chi' = 0.01$ compared with the smoothed exact solution: LCP.

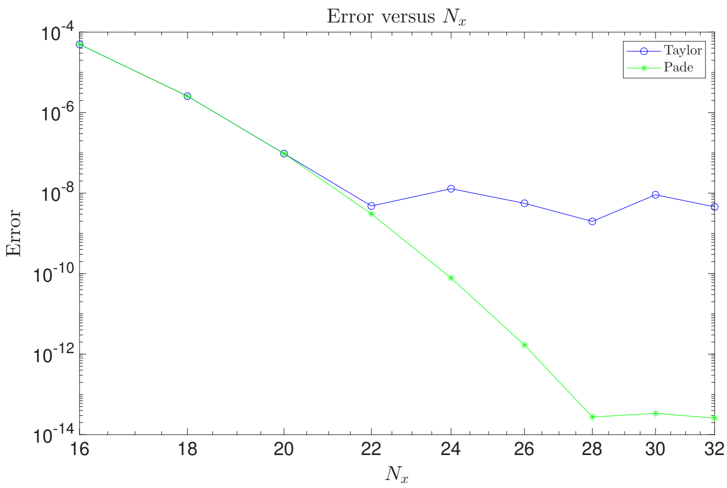

Fig. 12: Error versus N_x for $\chi' = 0.01$ compared with the smoothed exact solution: RCP.

10 Conclusion

In this work we have considered the interaction of electromagnetic waves with a periodic chiral structure. We focused on the special case of a uniform permeability/permeability, y–invariant structure with incident radiation aligned with this axis. In this case the governing equations can be decoupled into Left–

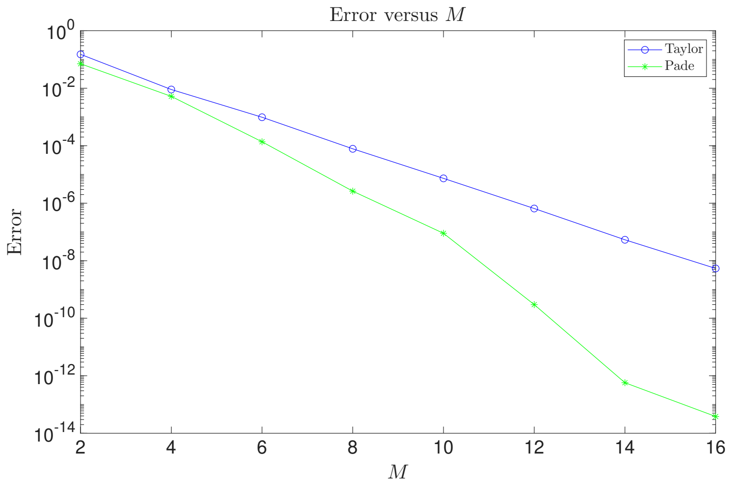

Fig. 13: Error versus M for $\chi' = 0.01$ compared with the smoothed exact solution: LCP.

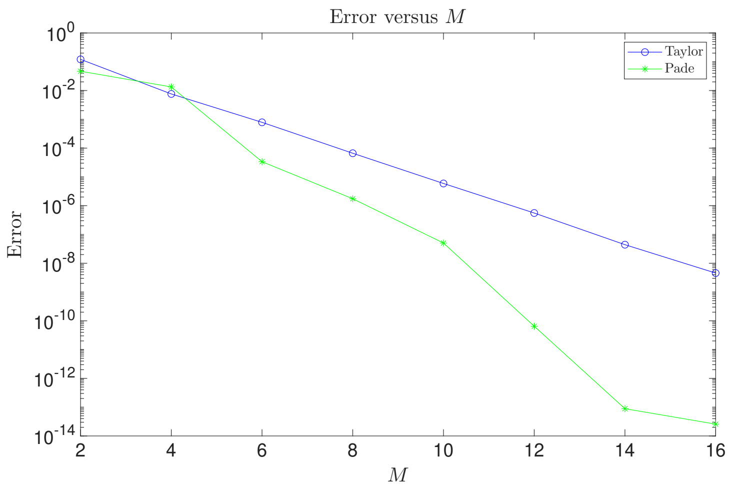

Fig. 14: Error versus M for $\chi' = 0.01$ compared with the smoothed exact solution: RCP.

and Right–Circular polarizations (LCP/RCP) for *scalar* fields, and we have proposed a High–Order Perturbation of Envelopes (HOPE) approach for their solution. We established two novel results: First, that these LCP/RCP fields are not only analytic in small envelope deformation, but also have a domain of analyticity which includes the entire real axis. Additionally, we showed that the fields depend *jointly* analytically upon the deviation parameters and the

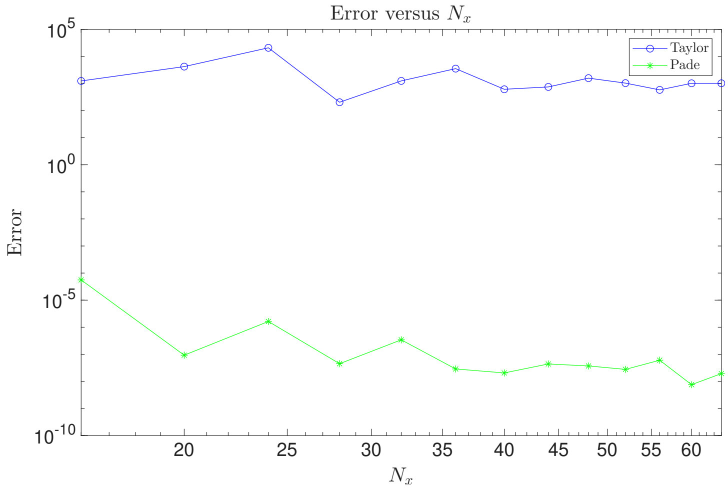

Fig. 15: Error versus N_x for $\chi' = 0.04$ compared with the smoothed exact solution: LCP.

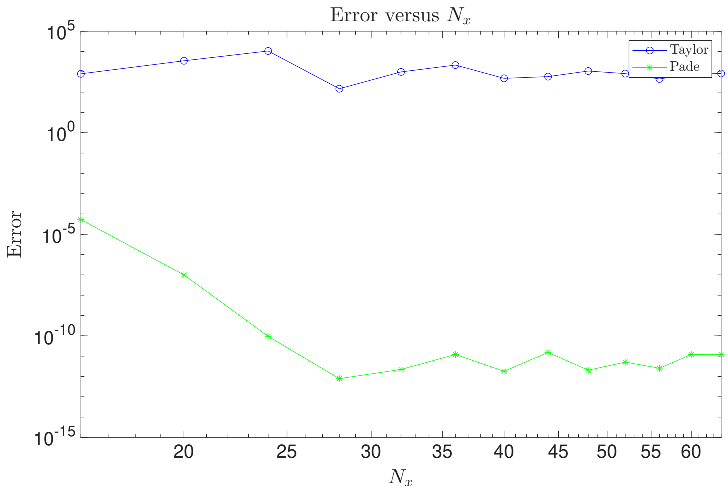

Fig. 16: Error versus N_x for $\chi' = 0.04$ compared with the smoothed exact solution: RCP.

spatial variables. Beyond this we demonstrated how a numerical implementation of this HOPE algorithm can be used to approximate solutions in a rapid, robust, and reliable manner.

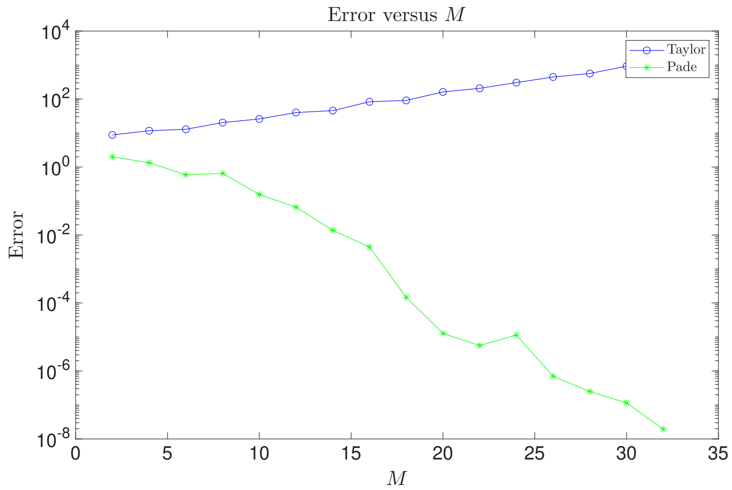

Fig. 17: Error versus M for $\chi' = 0.04$ compared with the smoothed exact solution: LCP.

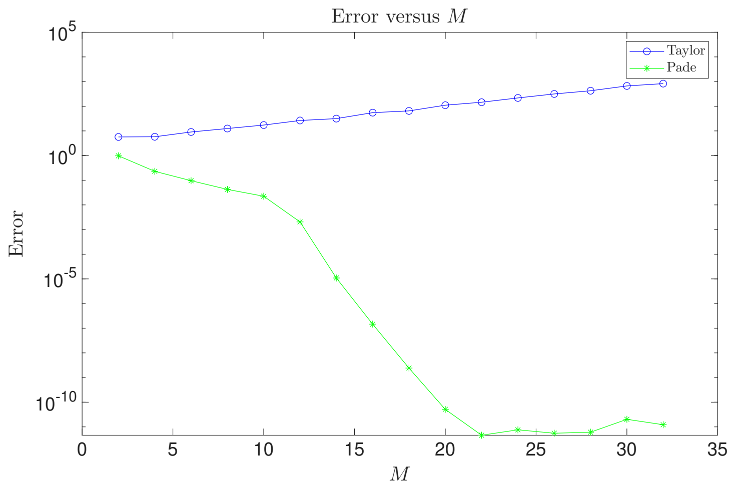

Fig. 18: Error versus M for $\chi' = 0.04$ compared with the smoothed exact solution: RCP.

Acknowledgments

D.P.N. gratefully acknowledges support from the National Science Foundation through grant No. DMS–2111283.

Declarations

Conflict of interest. The authors have no relevant financial or non-financial interests to disclose.
Author contributions. All authors contributed to the study conception and design. Material preparation, data collection and analysis were performed by all authors. The first draft of the manuscript was written by David P. Nicholls and all authors commented on previous versions of the manuscript. All authors read and approved the final manuscript.
Data Availability. The datasets generated during and/or analyzed during the current study are available from the corresponding author on reasonable request.

References

1. Ammari, H., Bao, G.: Analysis of the diffraction from periodic chiral structures. C. R. Acad. Sci. Paris Sér. I Math. **326**(12), 1371–1376 (1998)
2. Ammari, H., Bao, G.: Maxwell's equations in periodic chiral structures. Math. Nachr. **251**, 3–18 (2003)
3. Ammari, H., Bao, G.: Coupling of finite element and boundary element methods for the scattering by periodic chiral structures. J. Comput. Math. **26**(3), 261–283 (2008)
4. Arens, T.: Scattering by biperiodic layered media: The integral equation approach. Habilitationsschrift, Karlsruhe Institute of Technology (2009)
5. Athanasiadis, C., Costakis, G., Stratis, I.G.: Electromagnetic scattering by a homogeneous chiral obstacle in a chiral environment. IMA journal of applied mathematics **64**(3), 245–258 (2000)
6. Athanasiadis, C., Martin, P.A., Stratis, I.G.: Electromagnetic scattering by a homogeneous chiral obstacle: boundary integral equations and low-chirality approximations. SIAM Journal on Applied Mathematics **59**(5), 1745–1762 (1999)
7. Babaev, E., Kharzeev, D., Larsson, M., Molochkov, A., Zhaunerchyk, V.: Chiral Matter. WORLD SCIENTIFIC (2023). DOI 10.1142/13107
8. Baker Jr., G.A., Graves-Morris, P.: Padé approximants, second edn. Cambridge University Press, Cambridge (1996)
9. Bao, G., Li, P.: Maxwell's equations in periodic structures, *Applied Mathematical Sciences*, vol. 208. Springer, Singapore; Science Press Beijing, Beijing (2022)
10. Bender, C.M., Orszag, S.A.: Advanced mathematical methods for scientists and engineers. McGraw-Hill Book Co., New York (1978). International Series in Pure and Applied Mathematics
11. Blaschke, G., Kraft, H., Fickentscher, K., Köhler, F.: Chromatographische racemattrennung von thalidomid und teratogene wirkung der enantiomere [chromatographic separation of racemic thalidomide and teratogenic activity of its enantiomers (author's transl)]. Arzneimittelforschung **29**(10), 1640–2 (1979)
12. Boyd, J.P.: Chebyshev and Fourier spectral methods, second edn. Dover Publications Inc., Mineola, NY (2001)
13. Busch, K., König, M., Niegemann, J.: Discontinuous Galerkin methods in nanophotonics. Laser & Photonics Reviews **5**(6), 773–809 (2011)
14. Cossy, J. (ed.): Comprehensive Chirality (Second Edition), second edn. Academic Press, Oxford (2024)
15. Draine, B.T., Flatau, P.J.: Discrete-dipole approximation for scattering calculations. J. Opt. Soc. Am. A **11**(4), 1491–1499 (1994)
16. Enoch, S., Bonod, N.: Plasmonics: From Basics to Advanced Topics. Springer Series in Optical Sciences. Springer, New York (2012)
17. Evans, L.C.: Partial differential equations, second edn. American Mathematical Society, Providence, RI (2010)

18. Feng, L., Wang, H., Zhang, L.: The forward and inverse problems for the scattering of obliquely incident electromagnetic waves in a chiral medium. Journal of Differential Equations **284**, 102–125 (2021)
19. Gallinet, B., Butet, J., Martin, O.J.F.: Numerical methods for nanophotonics: Standard problems and future challenges. Laser and Photonics Reviews **9**, 577–603 (2015)
20. Gerlach, T.: The two-dimensional electromagnetic inverse scattering problem for chiral media. Inverse Problems **15**(6), 1663–1675 (1999)
21. Gottlieb, D., Orszag, S.A.: Numerical analysis of spectral methods: theory and applications. Society for Industrial and Applied Mathematics, Philadelphia, Pa. (1977). CBMS-NSF Regional Conference Series in Applied Mathematics, No. 26
22. Grogan DP, W.N.: Thalidomide. StatPearls Publishing, Treasure Island, FL (2023)
23. Guo, J., Wang, H.: On the direct and inverse electromagnetic scattering by chiral media. Journal of Differential Equations **317**, 495–523 (2022)
24. Homola, J.: Surface plasmon resonance sensors for detection of chemical and biological species. Chemical Reviews **108**(2), 462–493 (2008)
25. Jackson, J.D.: Classical electrodynamics, second edn. John Wiley & Sons Inc., New York (1975)
26. Jeong, H.H., Mark, A.G., Alarcón-Correa, M., Kim, I., Oswald, P., Lee, T.C., Fischer, P.: Dispersion and shape engineered plasmonic nanosensors. Nature Communications **7**(1), 11331 (2016). DOI 10.1038/ncomms11331
27. Jin, J.: The finite element method in electromagnetics, second edn. Wiley-Interscience [John Wiley & Sons], New York (2002)
28. Johnson, S.G., Joannopoulos, J.D.: Block-iterative frequency-domain methods for Maxwell's equations in a planewave basis. Opt. Express **8**(3), 173–190 (2001)
29. Khaliq, H.S., Nauman, A., Lee, J.W., Kim, H.R.: Recent progress on plasmonic and dielectric chiral metasurfaces: Fundamentals, design strategies, and implementation. Advanced Optical Materials **11**(16), 2300644 (2023)
30. Kim, H., Park, J., Lee, B.: Fourier modal method and its applications in computational nanophotonics. CRC Press, Boca Raton, FL (2012)
31. Kim, R.M., Huh, J.H., Yoo, S., Kim, T.G., Kim, C., Kim, H., Han, J.H., Cho, N.H., Lim, Y.C., Im, S.W., Im, E., Jeong, J.R., Lee, M.H., Yoon, T.Y., Lee, H.Y., Park, Q.H., Lee, S., Nam, K.T.: Enantioselective sensing by collective circular dichroism. Nature **612**(7940), 470–476 (2022). DOI 10.1038/s41586-022-05353-1. URL https://doi.org/10.1038/s41586-022-05353-1
32. Kress, R.: Linear integral equations, third edn. Springer-Verlag, New York (2014)
33. Kumar, J., Eraña, H., López-Martínez, E., Claes, N., Martín, V.F., Solís, D.M., Bals, S., Cortajarena, A.L., Castilla, J., Liz-Marzán, L.M.: Detection of amyloid fibrils in Parkinson's disease using plasmonic chirality. Proceedings of the National Academy of Sciences **115**(13), 3225–3230 (2018). DOI 10.1073/pnas.1721690115
34. Lakhtakia, A.: Beltrami Fields in Chiral Media. WORLD SCIENTIFIC (1994)
35. Lakhtakia, A., Varadan, V.K., Varadan, V.V.: Time-harmonic electromagnetic fields in chiral media, *Lecture Notes in Physics*, vol. 335. Springer-Verlag, Berlin (1989)
36. Lalanne, P., Morris, G.M.: Highly improved convergence of the coupled-wave method for TM polarization. J. Opt. Soc. Am. A **13**(4), 779–784 (1996)
37. Li, H., Ye, W., Polavarapu, L., Xie, J., Wong, K.Y., Zheng, G.: Chiral plasmonic superlattice resonance based on metasurfaces for chiral molecular sensors. Opt. Lett. **50**(9), 2900–2903 (2025). DOI 10.1364/OL.559690. URL https://opg.optica.org/ol/abstract.cfm?URI=ol-50-9-2900
38. Luo, T., Li, H., Zhang, Z., Wang, S., Pan, X., Mourdikoudis, S., Xue, C., Li, J., Wong, K.Y., Zheng, G.: Super-heterostructures of twisted Pd nanoarrays epitaxially grown on chiral Au nanorods boost circularly polarized photocatalysis. Advanced Science **12**(26), 2502848 (2025). DOI https://doi.org/10.1002/advs.202502848
39. Maier, S.A.: Plasmonics: Fundamentals and Applications. Springer, New York (2007)
40. Martin, O.J.F., Piller, N.B.: Electromagnetic scattering in polarizable backgrounds. Phys. Rev. E **58**, 3909–3915 (1998)
41. Meade, R.D., Rappe, A.M., Brommer, K.D., Joannopoulos, J.D., Alerhand, O.L.: Accurate theoretical analysis of photonic band-gap materials. Phys. Rev. B **48**, 8434–8437 (1993)

42. Moharam, M.G., Gaylord, T.K.: Rigorous coupled-wave analysis of planar-grating diffraction. J. Opt. Soc. Am. **71**(7), 811–818 (1981)
43. Moharam, M.G., Pommet, D.A., Grann, E.B., Gaylord, T.K.: Stable implementation of the rigorous coupled-wave analysis for surface-relief gratings: enhanced transmittance matrix approach. J. Opt. Soc. Am. A **12**(5), 1077–1086 (1995)
44. de Monvel, A.B., Shepelsky, D.: Direct and inverse scattering problem for a stratified nonreciprocal chiral medium. Inverse Problems **13**(2), 239–251 (1997)
45. Mun, J., Kim, M., Yang, Y., Badloe, T., Ni, J., Chen, Y., Qiu, C.W., Rho, J.: Electromagnetic chirality: from fundamentals to nontraditional chiroptical phenomena. Light: Science & Applications **9**, 139 (2020)
46. Nguyen, D.L.: The factorization method for the Drude–Born–Fedorov model for periodic chiral structures. Inverse Problems & Imaging **10**(2) (2016)
47. Nicholls, D.P.: A high–order perturbation of envelopes (HOPE) method for scattering by periodic inhomogeneous media. Quarterly of Applied Mathematics **78**, 725–757 (2020)
48. Nicholls, D.P., Reitich, F.: A new approach to analyticity of Dirichlet-Neumann operators. Proc. Roy. Soc. Edinburgh Sect. A **131**(6), 1411–1433 (2001)
49. Nicholls, D.P., Reitich, F.: Analytic continuation of Dirichlet-Neumann operators. Numer. Math. **94**(1), 107–146 (2003)
50. Nicholls, D.P., Taber, M.: Joint analyticity and analytic continuation for Dirichlet–Neumann operators on doubly perturbed domains. J. Math. Fluid Mech. **10**(2), 238–271 (2008)
51. Nicholls, D.P., Vo, L.: A high-order perturbation of envelopes (HOPE) method for vector electromagnetic scattering by periodic inhomogeneous media: Analytic continuation. Journal of Differential Equations **422**, 106–151 (2025)
52. Nicholls, D.P., Vo, L.: A high-order perturbation of envelopes (HOPE) method for vector electromagnetic scattering by periodic inhomogeneous media: Joint analyticity. SIAM Journal on Applied Mathematics **85**, 755–778 (2025)
53. Palyi, G.: Biological Chirality, first edn. Academic Press (2019)
54. Petit, R. (ed.): Electromagnetic theory of gratings. Springer-Verlag, Berlin (1980)
55. Potthast, R., Stratis, I.G.: On the domain derivative for scattering by impenetrable obstacles in chiral media. IMA journal of applied mathematics **68**(6), 621–635 (2003)
56. Raether, H.: Surface plasmons on smooth and rough surfaces and on gratings. Springer, Berlin (1988)
57. Rojas, R.: Integral equations for EM scattering by homogeneous/inhomogeneous two-dimensional chiral bodies. IEEE Proceedings-Microwaves, Antennas and Propagation **141**(5), 385–392 (1994)
58. Rumpf, R.: Electromagnetic and Photonic Simulation for the Beginner: Finite-Difference Frequency-Domain in MATLAB. Artech House, Inc., Boston, MA (2020)
59. Shen, J., Tang, T., Wang, L.L.: Spectral methods, *Springer Series in Computational Mathematics*, vol. 41. Springer, Heidelberg (2011). Algorithms, analysis and applications
60. Shull, P.J.: Nondestructive Evaluation: Theory, Techniques, and Applications. Marcel Dekker (2002)
61. Stratis, I.G.: Electromagnetic scattering problems in chiral media: a review. Electromagnetics **19**(6), 547–562 (1999)
62. Taflove, A., Hagness, S.C.: Computational electrodynamics: the finite-difference time-domain method, second edn. Artech House, Inc., Boston, MA (2000)
63. Taroudakis, M., Makrakis, G.: Inverse problems in underwater acoustics. Springer-Verlag, New York (2001)
64. Tokunaga, E., Yamamoto, T., Ito, E., Shibata, N.: Understanding the thalidomide chirality in biological processes by the self-disproportionation of enantiomers. Scientific Reports **8**(1), 17131 (2018). DOI 10.1038/s41598-018-35457-6. URL https://doi.org/10.1038/s41598-018-35457-6
65. Tsang, L., Kong, J.A., Shin, R.T.: Theory of Microwave Remote Sensing. Wiley, New York (1985)
66. Wang, S., Li, H., Fan, S., Chen, L., Zhou, H., Pérez-Juste, J., Pastoriza-Santos, I., Wong, K.y., Zheng, G.: Chiral plasmonic sensors: Fundamentals and emerging applications. Angewandte Chemie International Edition **64**(51), e202514816 (2025). DOI https://doi.org/10.1002/anie.202514816. URL https://onlinelibrary.wiley.com/doi/abs/10.1002/anie.202514816

67. Yeh, P.: Optical waves in layered media, vol. 61. Wiley-Interscience (2005)
68. Zhang, D., Guo, Y., Gong, C., Wang, G.: Numerical analysis for the scattering by obstacles in a homogeneous chiral environment. Advances in Computational Mathematics **36**(1), 3–20 (2012)
69. Zhang, D., Ma, F.: An inverse electromagnetic scattering problem for periodic chiral structures. Journal of Physics: Conference Series **12**(1), 180 (2005)
70. Zhang, D., Ma, F.: A finite element method with perfectly matched absorbing layers for the wave scattering by a periodic chiral structure. Journal of Computational Mathematics **25**(4), 458–472 (2007)